Post print of: Sedimentary Geology Volume 241, Issues 1-4, 15 November 2011, pages 22- 39

Elsevier Editorial System(tm) for Sedimentary Geology
Manuscript Draft

Manuscript Number: SEDGEO3988R1

Title: Chronology and tectono-sedimentary evolution of the Late Pliocene to Quaternary deposits of the Lower Guadalquivir foreland basin, SW Spain

Article Type: Research Paper

Keywords: Guadalquivir basin, Pliocene, Quaternary, foreland basin, forebulge, neotectonics

Corresponding Author: Dr Josep Maria Salvany,

Corresponding Author's Institution: Universitat Politècnica de Catalunya

First Author: Josep Maria Salvany

Order of Authors: Josep Maria Salvany; Juan Cruz Larrasoaña; Carlos Mediavilla; Ana Rebollo

Abstract: This paper presents new litho, chrono and magnetostratigraphic data from cores of 23 exploratory boreholes drilled in the Abalario and marshlands areas of the lower Guadalquivir basin (the western sector of the Guadalquivir foreland basin, SW of Spain). The lithologic logs of these boreholes identify four main sedimentary formations, namely: Almonte Sands and Gravels, Lebrija Clays and Gravels, Marismas Clays and Abalario Sands, respectively interpreted as proximal-alluvial, distal-alluvial, alluvial-estuarine and aeolian. From radiocarbon and magnetostratigraphic data, these formations were dated as Late Pliocene to Holocene. In the marshlands area, three main sedimentary sequences are present: a Late Pliocene-Early Pleistocene sequence of the Almonte and Lebrija (lower unit) formations, a Late Pleistocene-Early Holocene sequence of the Lebrija (upper unit) and Marismas formations, and a middle Holocene to present-day sequence of the upper Marismas Formation. The three sequences began as a rapid alluvial progradation on a previously eroded surface, and a subsequent alluvial retrogradation. In the third sequence, shallow estuarine and marsh sediments accumulated on top of the alluvial sediments. The aeolian sands of the Abalario topographic high developed coeval to alluvial and estuarine sedimentation after the first alluvial progradation, and continuously until the present. Correlation with the surrounding areas show that the sequences are the result of the forebulge uplift of the northern margin of the basin (Sierra Morena) and the adjacent Neogene oldest sediments of their northern fringe, both form the main source area of the study formations. This uplift occurred simultaneous to the flexural subsidence (SSE tilting) of the southern part of the basin, where sedimentary aggradation dominated.

Chronology and tectono-sedimentary evolution of the Late Pliocene to Quaternary deposits of the lower Guadalquivir foreland basin, SW Spain

Josep Maria Salvany [1], Juan Cruz Larrasoaña [2], Carlos Mediavilla [3], Ana Rebollo [3]

[1] Dept. Enginyeria del Terreny, Universitat Politècnica de Catalunya, c/ Gran Capità s/n, D2, 08034 Barcelona (Spain). E-mail: josepm.salvany@upc.edu

[2] Institut de Ciències de la Terra "Jaume Almera", CSIC, c/ Solé i Sabarís s/n, 08028 Barcelona (Spain). Now at: Area de Cambio Global, Instituto Geológico y Minero de España, Oficina de Proyectos de Zaragoza, C/ Manuel Lasala 44, 9B, 50006 Zaragoza (Spain)

[3] Instituto Geológico y Minero de España, Plaza de España, Torre Norte, 41013 Sevilla (Spain)

Correspondance addressed to JM Salvany

ABSTRACT

This paper presents new litho, chrono and magnetostratigraphic data from cores of 23 exploratory boreholes drilled in the Abalario and marshlands areas of the lower Guadalquivir basin (the western sector of the Guadalquivir foreland basin, SW of Spain). The lithologic logs of these boreholes identify four main sedimentary formations, namely: Almonte Sands and Gravels, Lebrija Clays and Gravels, Marismas Clays and Abalario Sands, respectively interpreted as proximal-alluvial, distal-alluvial, alluvial-estuarine and aeolian. From radiocarbon and magnetostratigraphic data, these formations were dated as Late Pliocene to Holocene. In the marshlands area, three main sedimentary sequences are present: a Late Pliocene-Early Pleistocene sequence of the Almonte and Lebrija (lower unit) formations, a Late Pleistocene-Early Holocene sequence of the Lebrija (upper unit) and Marismas formations, and a middle Holocene to present-day sequence of the upper Marismas Formation. The three sequences began as a rapid alluvial progradation on a previously eroded surface, and a subsequent alluvial retrogradation. In the third sequence, shallow estuarine and marsh sediments accumulated on top of the alluvial sediments. The aeolian sands of the Abalario topographic high developed coeval to alluvial and estuarine sedimentation after the first alluvial progradation, and continuously until the present. Correlation with the surrounding areas show that the sequences are the result of the forebulge uplift of the northern margin of the basin (Sierra Morena) and the adjacent Neogene oldest sediments of their northern fringe, both form the main source area of the study formations. This uplift occurred simultaneous to the flexural subsidence (SSE tilting) of the southern part of the basin, where sedimentary aggradation dominated.

Keywords: Guadalquivir basin, Pliocene, Quaternary, foreland basin, forebulge, neotectonics

1. Introduction

The lower Guadalquivir basin constitutes the sector of the Guadalquivir foreland basin located southwest of Sevilla (Fig. 1). Late Pliocene to Quaternary sediments in this sector of the basin mainly accumulated in two areas, namely the Guadalquivir marshlands and the Abalario high. The Guadalquivir marshlands form a wide flat area, of about 1800 km^2, located a few metres above the sea level in the western and lowest part of the Guadalquivir basin. In this area, the most recent part of the sedimentary filling consists of a sequence of flat-lying Plio-Quaternary deposits, up to 400 m thick, that accumulated from alluvial, estuarine and marsh sedimentary environments. The shallowest sediments of this sequence, which are mainly Holocene in age, have been extensively studied by Menanteau (1979), Zazo et al. (1994, 1999a), Rodríguez-Ramírez (1998), Rodríguez-Ramírez et al. (1996a, 1996b, 2001), Lario et al. (2001, 2002), Carretero et al. (2002), Ruiz et al. (2004, 2005), and Pozo et al. (2008, 2010). These authors made a detailed reconstruction of the sedimentary environments, discussed their evolution with regards to climate and sea-level changes, and provided a robust chronological framework based on radiocarbon dating. To the west of the Guadalquivir marshlands, the Abalario constitutes a coastal topographic high of about 450 km^2, made up by aeolian sands that are Late Pleistocene to Holocene in age. These sands crop out along the up to 100 m high and 30 km long Asperillo coastal cliff. The stratigraphic, sedimentologic and petrologic features of this cliff have been the focus of the studies by Caratini and Viguier (1973), Leyva and Pastor (1976), Flor (1990), Borja and Díaz del Olmo (1992), Dabrio et al. (1996), and Zazo et al. (1999b, 2005, 2008). The Abalario sands extend over the southernmost part of the Guadalquivir marshlands, constituting the currently active Doñana spitbar (Rodríguez-Ramírez et al., 1996b).

Bellow these more recent sediments, which constitute the Guadalquivir marshlands and the Abalario high, there is a less known sequence of Pliocene and early

Quaternary sediments drilled during several hydrogeology campaigns (FAO, 1970; IRYDA, 1976; IGME, 1983). Knowledge on these sediments is, however, restricted to their basic lithostratigraphic characteristics (Salvany and Custodio, 1995) for the following reasons: 1) the destructive method used to drill the boreholes, which enabled just a rough description of the sediments recovered; 2) the unequal distribution of boreholes, which are concentrated in the northwestern part of the marshlands (irrigated land) but are almost absent along the eastern margin of the Guadalquivir River (area of brackish groundwater) and the linking zone with the Abalario high (restricted area of the Doñana National Park), thus preventing a detailed correlation between different areas. Such correlation became even more difficult because of the frequent and complex lateral changes in sedimentary facies; and 3) the lack of biostratigraphic markers, which prevent development of an independent chronostratigraphic framework.

During the last decade, the IGME (Geological and Mining Institute of Spain) has drilled several exploratory boreholes in different points of the Guadalquivir marshlands and the Abalario high (Fig. 1) in an effort to gain insights on the lithostratigraphy, sedimentology and chronology of the Plio-Quaternary sediments. Most of these boreholes, which reach down to 300 m, were drilled with continuous core sampling to recover unaltered material suitable for detailed sedimentary studies. In this paper we present the first detailed description of the sediments in these boreholes, define lithostratigraphic units, and bring new chronologic data based on radiocarbon and magnetostratigraphic dating. This information, combined with a complete revision of the older hydrogeological boreholes, is used to propose a new lithostratigraphic and chronologic framework for the whole Plio-Quaternary sedimentary sequence and to establish the paleogeographic evolution of the western part of the Guadalquivir basin in its geodynamic context as the foreland of the Betic Cordillera.

2. Geological setting

The Guadalquivir basin in southern Spain is an ENE-WSW elongated foreland basin developed during the Neogene and Quaternary between the external zones of the Betic Cordillera to the south and Sierra Morena (Iberian Massif) to the north (Sanz de Galdeano and Vera, 1992), which respectively form its active and passive margins (Fig. 1). The basin started to develop during the Middle Miocene in response to flexural subsidence of the Iberian Massif caused by the stacking of allochthonous units of the Betic Cordillera during the convergence between the Iberian and African plates (Sierro et al., 1996; Fernández et al., 1998; Civis et al., 2004; García-Gastellanos et al., 2002). The external zones of the Betic Cordillera are made up of Mesozoic and Cenozoic sediments that include thick calcareous and evaporitic formations, as well as siliciclastic units. Sierra Morena comprises in Paleozoic igneous and metamorphic rocks. These rocks constitute the basement of the Guadalquivir basin, which gradually increases its depth toward the SSE so that it is found 5000 m below the Betic thrust front (Fernández et al., 1998; García-Castellanos et al., 2002).

In the lower Guadalquivir basin, the lowermost unit of the sedimentary filling of the basin is the Niebla Calcarenite Formation (Civis et al., 1987; Baceta and Pendón, 1999). This formation is made up of up to 30 m of gravel, fossil-bearing sand and limestone accumulated in alluvial and coastal environments. It covers an old erosive surface on the Paleozoic basement. The Niebla Calcarenite Formation is overlain by the Gibraleón Clays Formation (Civis et al. 1987), also know in the literature as Blue Marls, which forms a monotonous marly sequence accumulated in a deep marine through formed at the foothill of the Betic Cordillera. This formation increases its thickness from the northern margin of the basin, where it reaches a few tens of metres, to its southern margin, where it reaches more than 1000 m and includes subordinate sand beds (Perconig and Martínez-Díaz, 1977; Martínez del Olmo et al., 2005). This thicker part hosts the so-called allochthonous units (traditionally called “olistostromic units”), which consist of Triassic evaporites and are related to thrusting along the Betic Cordillera deformation front (Berástegui et al., 1998). The Gibraleón Clays Formation is overlain by the Huelva Sands Formation (Civis et al., 1987), made up by up to a few tens of metres of fossil-rich marls, sands and sandstones accumulated in a shallow marine environment. The Huelva Sands Formation is overlain by the Bonares Sands Formation (Mayoral and Pendón, 1986-87), made up by up to a few tens of metres of sands and subordinate levels of gravels accumulated in a coastal environment. The abundant microfaunal content of the upper part of the Niebla (Civis et al., 1987), Gibraleón (Magne and Viguier, 1974; Sierro, 1985), and Huelva (Ruiz-Muñoz et al., 1997) formations has yielded Tortonian, Late Tortonian to Late Messinian, and Late Messinian to Early Pliocene ages for these formations, respectively. No biostratigraphic data are available for the Bonares Formation, tentatively dated as Middle-Late Pliocene-Early Quaternary on the basis of its stratigraphic position above the Huelva Formation (Mayoral and Pendón, 1986–87).

The overlying sediments, of uncertain Plio-Quaternary age, have a more varied geographical distribution and sedimentological significance. In the northern part of the basin, they form a characteristic red coarse alluvial deposit that caps the top of many hills and has a maximum thickness of about 10 m. This deposit was named High Alluvial Level by Pendón and Rodríguez-Vidal (1986–87) and Red Formation by Torres-Perezhidalgo et al. (1977a, 1977b), which are respectively located in the western part and the north-central part of the basin (Fig. 1). They also constitute the old alluvial terraces linked to the evolution of the current drainage network (Salvany, 2004). In the southern part of the basin, three main Plio-Quaternary units were early identified by Salvany and Custodio (1995) from borehole data: an older Alluvial Unit, made up of gravel, sand and clay, about 200 m thick, and two younger coeval units: the Marismas Unit, which is a clayey unit of estuarine origin of up to 60 m thick, and the Aeolian Unit, a sandy unit that reaches a thickness of 150 m. The development of these two younger units leads to the formation of the marshlands area and the Abalario high, respectively.

The structure of the Plio-Quaternary deposits of the lower Guadalquivir basin remains a controversial subject. Some authors identify two sets of normal faults linked to an assumed Pliocene extensional phase, namely a main group of N-S oriented faults that includes the lower Guadalquivir, Guadiamar and Odiel faults, and a subordinate system of E-W oriented faults that mainly developed in the westernmost part of the basin (Armijo et al, 1977, Viguier, 1977). Later studies by Goy et al. (1994, 1996) and Zazo et al. (1999a, 2005), describe similar faults that controlled the more recent sedimentation in coastal areas during the Quaternary. On the other hand, studies by Flores-Hurtado and Rodríguez-Vidal (1994) and Salvany (2004) describe a regional tilting of the basin toward the SSE as the dominant structural feature controlling the sedimentation, and do not identify the fault pattern envisaged by other authors.

3. Data and methods

3.1. Studied boreholes

We have studied the sedimentary sequence recovered from the 22 exploratory boreholes drilled by the IGME in the Guadalquivir marshlands and the Abalario high between 1999 and 2008 (Table 1, Fig. 1). The study is further completed with the VPL borehole (250 m deep) drilled in 2008 by a private company in the Veta La Palma property. These boreholes were mainly drilled by a direct circulation rotary method with continuous core sampling (Cruse, 1979). This method supplies unaltered material, enabling detailed lithologic logging, and is suitable for analytical determinations, such as radiocarbon and magnetostratigraphic dating. The occurrence of intervals made up by loose sand and gravel made this type of drilling unfeasible, so they were drilled using a roller bit with a direct circulation of fluids. In this case, cuttings come up through the annular space between the borehole and the rotating drill pipes, providing a mixture of sediments that might include material dragged from the borehole walls thus a rough identification of the lithology. Boreholes HT, CL and VPL were totally drilled by a roller bit of large diameter with a reverse circulation of fluids, where the cuttings come up inside the drill pipes lessening mixtures. This method generates cuttings large enough for a reasonably good description of the lithology but not for analytic determinations.

The 23 studied boreholes sum a total length of 5253.85 m. Except for HT, CL and VPL, 70.4% of the total borehole length corresponds to pristine sediments drilled with continuous core sampling, and the rest corresponds to cuttings drilled using other methods. This ratio varies between 100% in eight boreholes and 29.3% in borehole F1.

Additionally, the lithologic-logs of a total of 580 old hydrogeologic boreholes were revised. These boreholes were all drilled using a roller bit, some times with direct circulation and others with reverse circulation of fluids. They provide lithologic-logs of variable quality. In general, boreholes drilled with reverse circulation of fluids supplied lithological information of reasonable good quality for the purpose of our study.

The location of all lithostratigraphic and analytical data within the studied boreholes is marked by their position with respect to the surface and is referred to as metres below the surface (mbs).

3.2. Radiocarbon data

To date the uppermost sediments of the marshlands, a total of 17 samples of organic matter were analyzed using the ^{14}C method (Table 2). Samples were taken from different boreholes, where the organic remains appear as black layers of peat or scattered fragments of wood or charred material. In all cases, samples correspond to organic-rich material in enough amounts to ensure reliable data. This is especially the case in peat layers, where the organic matter is an abundant material easy to separate in the laboratory from its siliciclastic host sediment. The fragments of wood and charred material have common sizes up to few centimetres. Once separated from their host sediment, these isolated fragments become very pure organic remains of good quality for radiocarbon analysis.

Most of these samples were analysed following the AMS method in the Beta Analytic Laboratory in Florida (USA) and the Poznan Radiocarbon Laboratory in Poland. To support the paleomagnetic data described below, and in view of the important development of peat layers in its uppermost part, the LE borehole was sampled in more detail.

3.3. Paleomagnetic data

In order to provide a chronological constraint for the studied formations, we have performed a magnetostratigraphic study of the LE borehole. This borehole was chosen because it covers the most complete sequence of fine-grained Pliocene and Quaternary sediments suitable for paleomagnetic analyses, and includes the thickest sequence of recent marshlands deposits suitable for radiocarbon dating. A total of 98 paleomagnetic samples were drilled perpendicular to the borehole sections using a standard petrol-powered drill. Paleomagnetic sampling focused on fine-grained lithologies such as clays and fine-grained sands, and avoided coarser-grained lithologies, less useful for paleomagnetic analyses. The sampled section includes the whole uppermost 270 m of the LE borehole, with the exception of a 23 m interval of unconsolidated sands and gravels between 76 and 99 mbs. This has resulted in a homogeneous sampling with a mean resolution of about 2.1 m. Sediments below 270 mbs could not be drilled due to the unconsolidated nature of the mostly coarse bioclastic sands.

Paleomagnetic analyses were carried out using a 2G superconducting rock magnetometer at the Paleomagnetic Laboratory (SCT-UB/CSIC) of the Institute of Earth Sciences Jaume Almera in Barcelona (Spain). The noise level of the magnetometer is less than 7 x 10^{-6} A/m, much lower than the magnetization of the measured samples. Thermal treatment, which was conducted using a MMTD–80 furnace, involved between 8 and 12 steps at intervals of 100°, 50°, 30° and 20°C to a maximum temperature of 680°C. Demagnetization of a set of pilot samples representative of all the lithologies studied allowed optimizing the demagnetization steps and thus the accurate calculation of the magnetization directions that minimize the heating and formation of new magnetic phases in the oven. Stable Characteristic

Remanent Magnetization (ChRM) directions were identified through visual inspection of orthogonal demagnetization plots (Zijderveld, 1967), and were calculated by means of Principal Component Analysis (Kirschvink, 1980).

4. Results

4.1. Lithostratigraphy

The lithologic logs of the studied boreholes has enabled identification of a lower marine sequence, made up of fossil-bearing marly and sandy sediments of characteristic grey colour, and an upper continental to restricted marine sequence consisting in gravels, sands and clays that display a variety of colours and have a low marine fossil content. The first sequence includes the Neogene sediments of the Gibraleón and Huelva formations. The lithostratigraphy, sedimentology and chronology of these formations are described in detail in studies cited above, so they are not further discussed. The second sequence includes the overlying, newly defined Almonte, Lebrija, Abalario and Marismas formations, whose main lithological characteristics are described next.

4.1.1. Almonte Sands and Gravels Formation

This formation constitutes a coarse clastic unit made up by gravels, sands and occasional clayey and marly intervals, and is orange, yellow and, less frequently, grey (Figs. 2, 3 and 4). In the marshlands area, this unit has a thickness that increases southward from 10 to 110 m. In this same southward direction, the grain size of gravels tends to decrease, and the sediments grade from sandy gravels to dominant sands with minor gravel beds. Both gravels and sands are loose, lack a clayey matrix, and have grain shapes that range from well rounded to subangular. Gravel grains reach more than 10 cm in size, with more common grain sizes, between 1 and 5 cm. They are of metamorphic and igneous composition, dominantly quarzose in nature, although fragments of schists, hornfels and porphyrs are also present. Sand grains are mainly of quartz composition, with variable amounts of plagioclase, alkali feldspars, and rock fragments. This composition indicates that the source area was located north of the basin, in the Sierra Morena, because no metamorphic and igneous rocks are found in the Betic margin. The lower boundary of this formation is represented by a gradual transit from the underlying Huelva Formation in the south-eastern part of the marshlands (boreholes MA, PN, SL and LE). Toward the northern and western part of the marshlands, this boundary is an erosive surface developed on the Huelva Formation.

In the Abalario area, the Almonte Formation is a thin homogeneous layer that reaches 26 m thick in the LJ borehole (Fig. 2). It constitutes a fining-upward sequence with an erosive basal surface that cuts the underlying Huelva Formation. The fact that the alluvial sediments were not drilled in most of the boreholes, in the transition between the Abalario and the marshlands, suggests the existence of a gentle paleorelief originated during the down cutting phase previous to their sedimentation (Fig. 5, cross-section 5).

The Almonte Formation records the development of a wide, alluvial system that drained the Sierra Morena and extended beyond the current coastline. It represents the onset of continental deposition in the Guadalquivir basin, which followed the long episode of marine sedimentation persistent in the basin since the Tortonian (Late Miocene).

4.1.2. Lebrija Clays and Gravels Formation

This formation is made up of clays with subordinate sand and gravel beds that have a variable vertical distribution at different locations (Figs. 2, 3 and 4). The formation can be divided into two units. The lowermost one is made up by brown and greenish clays that have either a visually massive or a laminated structure. Massive clays contain common root marks and white carbonate nodules. Laminated clays are made up of an alternation of thin fine-grained sandy and clayey layers. Occasional marine shells of gastropods and bivalves are also found. Sands have a clayey matrix, range from fine to coarse grain size, and include subordinate gravel layers and many scattered mud-clasts. Gravels contain well-rounded clasts of up to 10 cm in size, and include variable fractions of a clayey and sandy matrix. Gravels form layers of several metres in thickness with a fining-upward structure, and have a rare lateral continuity between adjacent boreholes (paleochannels). Clasts and sand grains are dominantly quarzose and metamorphic in composition, similar to that described above for the Almonte Formation. This lower unit extends throughout the southern part of the studied area, and increases its thickness towards the southeast, reaching a maximum thickness of 120 m at the LE borehole (Fig. 3). In this borehole, the unit is directly overlying the Huelva Formation. However, towards the north and west, it gradually expands over the sediments of the Almonte Formation (Fig. 5).

Sediments of this lower unit can be interpreted as distal alluvial sediments accumulated on a muddy alluvial plain crossed by gravel-bearing fluvial channels sourced in the Sierra Morena. The root traces and carbonate nodules suggest wide spread development of vegetation on the muddy plain. Although the main sediments indicate an alluvial environment, occasional marine bivalve shells might indicate some sporadic marine influence in the southern part of the basin. This lower unit of the Lebrija Formation can be considered as the distal sediments of the Almonte alluvial system (Fig. 5).

The upper unit of the formation is a fining-upwards sequence of coarse gravels at the base, gravels and coarse-grained sands in the middle part, and coarse- to fine-grained sands towards the top. It forms a continuous bed throughout most of the northern half of the marshlands. In the northernmost boreholes (SE, MJ, F1 and F4), this unit cuts the Almonte Formation, while in the other boreholes it grades over the lower unit of the Lebrija Formation. In the northern part of the marshlands the upper unit has a rather constant thickness of 10 to 15 m that reaches 22 m at the LE borehole (Fig. 3). However, toward the south it becomes thinner (PN, VPL, MA boreholes) and it is even locally absent (VP) (Fig. 5). Again, the dominant quartzose and metamorphic composition of pebbles and sands indicate a northerly provenance in the Sierra Morena. Due to its loose and coarse-grained nature, sediments of this upper unit were drilled using the roller bit. Therefore, only a basic lithologic description based on cuttings is available.

Sediments of this upper unit can be interpreted as proximal alluvial sediments that throughout the northern part of the study area rapidly prograded over the Almonte Formation and the lower unit of the Lebrija Formation (Fig. 5).

4.1.3. Abalario Sands Formation

This formation (formerly the Aeolian Unit of Salvany and Custodio, 1995) is a thick package of homogenous medium- to fine-grained sands that lack of a clayey matrix and are white, yellow and orange (Figs. 2 and 4). Sands are mainly quartz, but include feldspars and heavy minerals that form thin, black laminae (Caratini and Viguier, 1973; Leyva and Pastor, 1976). The lack of fossils is another significant feature of their composition. Sands are occasionally cemented by iron oxides in nodules and hard crusts up to several centimetres thick, which have a characteristic reddish colour. The formation shows a maximum thickness of 150 m in the southeastern part of the Abalario high, and thins progressively to the north and west.

The sediments of the Abalario Formation originated from an aeolian system that prograded NW to SE following the shoreline. According to Caratini and Viguier (1973), the sands were supplied by reworking of the Late Pliocene sediments under denudation in the northern margin of the basin. The aeolian origin of these sediments was mainly documented in the Asperillo coastal cliff. Along this cliff, typical aeolian cross-beds are exposed together with thin iron-oxide crusts, paleosoils and carbon-rich layers (Flor, 1990; Borja and Díaz del Olmo, 1992; Dabrio et al., 1996; Zazo et al., 2005). The cliff cuts ancient dunes originally developed several hundred of metres inland. Related beaches of this aeolian system were completely eroded by the sea waves and reworked into the spitbar of Doñana (Rodríguez-Ramírez, 1998). Bellow the cliff, the lower sands of the Abalario Formation display the same lithofacies. This suggest that the aeolian system developed continuously from the beginning of the formation, first covering the alluvial sediments of the Almonte Formation and then onlapping over the lateral equivalents of the Lebrija and Marismas formations (Fig. 5, cross-section 5). Such lateral gradation is supported by the sediments drilled between the Abalario and the marshlands at boreholes TC, SO, and CL, where aeolian sands intercalate frequent grey or greenish clay beds, often with carbonate nodules, root molds and vegetal remains that are wedges of the adjacent Lebrija and Marismas clayey formations. Today, aeolian dunes are only active at the Doñana spitbar. Elsewhere the aeolian areas are inactive and are being eroded (Flor, 1990; Dabrio et al., 1996).

4.1.4. Marismas Clays Formation

This formation is made up of a characteristic dark grey or brown homogenous clay that includes minor clayey sandy layers of fine to medium grain size (Figs. 2, 3 and 4). The clays and sands commonly are laminated and contain organic matter. Shells of bivalves, gastropods, echinoderms, and other marine fauna are commonly found scattered or concentrated in coquina layers several centimetres thick. Closed bivalve shells are often found along with unbroken shells of other marine fauna, indicating a very low energy environment. Organic mater appears either diffuse within the sediments or concentrated in peat layers of few centimetres thick. Black vegetal roots and wood fragments are also frequently scattered within these sediments. Occasional paleochannels of gravel and coarse-grained sand interbedded within the clays are present in the LE and HT boreholes.

The thickness of the Marismas formation gradually increases from north to south, from less than 20 m in boreholes MJ and SE to 79 m in LE borehole (Figs. 2 and 3). The sand content increases significantly in the same direction, even to the point of exceeding the clay fraction. The lower boundary of this formation in the central part of the Guadalquivir marshlands is a gradual contact over the underlying upper unit of the Lebrija Formation. As a local feature, the Marismas clays reach a large development in the south-eastern edge of the marshlands (borehole CM, Figs. 4 and 5). In this case, it is considered that a substantial part of this sequence could represent a lateral gradation of the more distal sediments of the Lebrija Formation. The upper boundary of the Marismas Formation corresponds to the surface of the marshlands, where sedimentation continues.

The Marismas Formation represents a marine transgression that expanded over the previously deposited alluvial sediments of the Lebrija Formation. It is a shallow marine deposit that filled an estuary developed in the present-day marshland area. Clay intervals can be interpreted as muddy lagoon sediments, while sands would represent sandbars, beaches or sandlflats developed around the lagoon. In the north-western part of the marshlands (boreholes MJ, F1, F4 and HT), the Marismas Formation forms a homogenous clayey sequence that suggests the development of a relatively stable lagoon. In the eastern part of the marshlands (boreholes VPL, VP, LE, PE and SE), the Marismas Formation constitutes a transgressive sequence made up with a lower sand layer, without fossil remains; an intermediate interval, where marine shell-bearing clay and sand layers alternate, and an upper clayey layer that contains common marine shell. The lower sands of this sequence can be interpreted as distal alluvial sediments coming from the northern part of the basin (the mouth of the early Guadalquivir River). Upward, marine sediments gradually developed, first as sandflat and beach sediments and later as lagoon sediments. In the southern part of the marshlands, the Marismas Formation constitutes a sandy sequence with minor clayey layers (boreholes PN and MA). Toward the south-east, sand layers become less frequent (borehole SL), even non-existent (borehole CM). This area can be interpreted as a coastal sandy barrier that prograded toward the SE. The barrier sands were supplied by reworking the aeolian sands of the Abalario area. This source agrees with the similar quarzose composition of both the Abalario and Marismas sands. Development of this barrier leads to the formation of the spitbar of Doñana, which closed the estuary and formed the present-day marshlands.

4.2. Radiocarbon data

All samples located at less than 40 mbs in every borehole sampled have radiocarbon ages younger than 9600 ± 50 years BP (Table 2). Two additional samples located between 50 and 60 mbs in the VP and TC boreholes have ages ranging from 29880 ± 280 to 45460 ± 1900 years BP. At levels deeper than 60 mbs, all available ages are beyond the range of radiocarbon dating. The exception to this pattern is the PN borehole, where ages beyond the range of the radiocarbon method are found at a depth of 35.5 mbs (Table 2).

4.3. Magnetostratigraphy

In most samples, two stable components are present. A low-temperature component is unblocked below 225–300ºC. This component shows either steep directions of around 50–60º (Fig. 6 A, C), interpreted as present-day field overprints, or shallow directions broadly perpendicular to the borehole sections (Fig. 6 D, I), interpreted as acquired during drilling. Above 225–300ºC, a ChRM can be identified in about 95% of the samples. The behaviour of the ChRM depends on lithology. The ChRM in grey clays and fine-grained sands from the Marismas and Huelva formations shows maximum unblocking temperatures of up to 500º C (Fig. 6 A, B, G, I), which points to magnetite as the main magnetic carrier. In clays and fine-grained sands from the Lebrija Formation, the maximum unblocking temperature of the ChRM ranges between 420º and 650º C, indicating that hematite is also a common magnetic carrier.

Based on demagnetization pattern, ChRM directions were divided into three groups. Type 1 ChRMs are those that describe well-defined linear trends that enable the accurate calculation of their directions and optimum polarity determinations (Fig. 6

A, C, E, G). Type 2 ChRMs are those that either display less-developed linear trends or incomplete demagnetizations due to the growing of new magnetic minerals in the oven. Nevertheless, they provide reliable polarity determinations by fitting selected or clustered directions to the origin of demagnetization plots (Fig. 6 D, F, H). Type 3 ChRMs are those that display clustered directions that might provide ambiguous polarity determinations (Fig. 6 I). About 43, 42 and 15% of ChRM directions belong to Quality Types 1, 2, and 3, respectively.

ChRM shows both positive and negative inclinations regardless of lithology. The mean of the negative ChRM directions is –38.9º ± 21.2º, a few degrees shallower than the mean of the ChRM normal directions (+45.9º ± 20.2º) and likely results from a stronger overlap of negative ChRM directions with the present-day field overprint. The means of both positive and negative ChRM directions are slightly shallower than the expected inclination for the studied site (around ±50º), which is consistent with a detrital origin for ChRM. In any case, both positive and negative ChRM mean directions are statistically consistent with the expected inclination, which suggests, together with the lack of a lihological control on ChRM directions, that ChRM provides a reliable record of the polarity reversals of the geomagnetic field.

Because the azimuth of the borehole is unknown, plus the need for quality, the identification of polarity zones was solely based on the inclination of Type 1 and 2 ChRM directions (Fig. 7). Nevertheless, most Type 3 ChRM directions appear to be consistent with those of Types 1 and 2. The established succession of polarity reversals includes 5 normal magnetozones, here labelled N1 to N5 from top to bottom, and 5 reverse magnetozones, here labeled R1 to R5 (Fig. 8). Each magnetozones was determined by at least two consecutive samples, averaging a total of 7.8 samples per magnetozone. Short intervals of only one sample, which might correspond to chryptochrons, were not considered. The most conspicuous patterns of the Lebrija borehole polarity sequence are a long normal polarity interval in the upper part of the section (N1), two reverse magnetozones (R1, R2) separated by a short normal interval

(N2) in the centre of the section, and a cluster of three short normal magnetozones (N3 to N5) separated by two short reverse intervals (R3, R4) in its lower part (Fig. 7).

5. Discussion

5.1. Chronology of the Plio-Quaternary sedimentary sequence

Radiocarbon data enable identification of Holocene ages (i. e., < 11.5 Ka BP) to a depth of 17.5, 28.9 and 37.6 mbs in PN, PE and LE boreholes, respectively (Table 2). On the other hand, Late Pleistocene ages of 29880 ± 280 and 45460 ± 1900 years BP are found at depths between 50 and 60 mbs in TC and VP boreholes. Bellow 60 mbs, all ages are beyond the range of radiocarbon dating. In an earlier study, Zazo et al. (1999a) provided three radiocarbon ages from shells from the Mari López borehole, drilled in the Guadalquivir marshlands 6 km southwest of HT borehole. Two samples taken at 7.3 and 10.8 mbs gave Holocene ages younger than 6000 years BP, whereas a third sample collected at 27.5 mbs gave a Late Pleistocene age of 47400 ± 3100 years BP. The study by Pozo et al. (2010) provided five radiocarbon ages from shells from the PLN (Palacio de Las Nuevas) borehole, close to the PN borehole of our study. Four samples, taken above 25 mbs gave Holocene ages younger than 7000 years BP. The fifth sample collected at 55.3 mbs gave a Late Pleistocene age of 43370 ± 960 years BP. Additional radiocarbon ages from shells of less than 5000 years BP taken from the shallowest sediments of the southwest area of the marshlands were provided by Ruiz et al. (2004 and 2005).

Overall, these results place the Pleistocene-Holocene boundary within the Marismas Formation deeping eastward from around 11 mbs in the Mari López borehole (Zazo et al., 1999a) to 40 mbs in the Lebrija borehole (LE). They also indicate that ages beyond the range of radiocarbon dating, and hence older than approximately 50000 years BP, are present at variable depths between about 30 mbs in the Mari López and PN boreholes and 60 m in LE, VP, and TC boreholes.

The correlation of the polarity sequence established for LE borehole with the revised astronomically-tuned Neogene timescale (ATNTS2004 of Lourens et al., 2004 and Gradstein et al., 2004) is straightforward based on the characteristic pattern of magnetozones, on available radiocarbon ages for the Marismas Formation, and on biostratigraphic constraints for the Huelva Formation. Radiocarbon ages of < 11.5 Kyr BP in the uppermost part of the long N1 interval constraint it to correlate with those of Brunhes (C1n) chron (Fig. 7). This implies that the underlying, predominantly reverse interval (R1 to R2) must correlate with the Matuyama period (chrons C1r to C2r), so that the characteristic cluster conformed by intervals N3 to N5 corresponds to the predominantly normal Gauss (C2.An) chron and the underlying R5 interval correlates to the top of the Gilbert (C2Ar) period. This correlation is supported by biostratigraphic data indicating an Early Pliocene age for the Huelva Formation (Sierro et al., 1996). The short N2 interval can be correlated either to the Jaramillo (C1r.1n) or to the Olduvai (C2n) events of the Matuyama period (Fig. 7). Since no evidence of a sedimentary hiatus was observed in the upper part of the upper unit of the Lebrija Formation, the best match is provided by the correlation of N2 to the Olduvai chron (Fig. 7). This interpretation implies that most of chron C1r (including the Jaramillo event) is either missing below, or represented within the 22 metres-thick package of unconsolidated gravels and coarse-grained sands that made up the upper unit of the Lebrija Formation.

The radiocarbon and magnetostratigraphic results enable determinating the ages and mean accumulation rates for the formations, and estimating on the age and duration of the sedimentary gap around the upper unit of the Lebrija Formation (Fig. 7). Mean accumulation rates of about 350 cm/Kyr for the Holocene part of the Marismas Formation in LE borehole can be estimated keeping in mind the position of the Pleistocene-Holocene boundary at about 40 mbs. Toward the west, this accumulation rate decreases down to about 95 cm/Kyr as the depth of the Pleistocene-Holocene boundary reaches shallower positions of around 11 mbs (i. e., Mari López borehole).

For the lower part of the Marismas Formation, a mean accumulation rate of about 50 cm/Kyr can be established for all boreholes on the basis of location, at variable depths between 30 (in the Mari López and PN boreholes) and 60 mbs (in LE, VP, and TC boreholes), of ages beyond the range of radiocarbon dating. The linear extrapolation of this accumulation rate downwards from the position of the Pleistocene-Holocene boundary results in an estimated Late Pleistocene age between 85 and 110 Ka for the base of the Marismas Formation.

Concerning the Lebrija Formation, the age of its base can be constrained at ~3.7 Ma. A mean accumulation rate of around 6 cm/Kyr can be established for this formation between the lower boundary of chron C2An and the top of the Olduvai chron (C2n) in LE borehole. However, these are just mean accumulation rates that might have larger and smaller values. This situation is clearly illustrated in the lower part of the formation, where the presence of several polarity reversals within chron C2An demonstrates that accumulation rates oscillate from <1 to >10 cm/Kyr. Something similar is found between 99 and 110 mbs, where the presence of the Olduvai chron enables estimating accumulation rates as low as 1.2 cm/Kyr. Such highly variable accumulation rates over short time intervals are attributed to the nature of the coarse-grained intervals within the Lebrija Formation, which are characterized by channel-like geometries involving periods of either erosion or no deposition. The extrapolation of the linear accumulation rates upwards from the top of the Olduvai event in LE borehole yields an estimated age of about 1.6 Ma for the top of the lower unit of the formation (Fig. 7). In view of the transitional contact between the top of the upper unit of the Lebrija Formation and the base of the Marismas Formation, which is dated at about 100 Ka, a period of up to ca. 1.6 Myr must be represented either within or at the base of its upper unit. It is unknown whether this time interval was accommodated by a period of deposition followed by erosion or by a period with very low but continuous agraddation. Given the sharp lower boundary of the upper unit of the Lebrija Formation, and keeping in mind that it represents a widespread expansion of alluvial sedimentation over different underlying formations, the first option seems more likely. In that case, an age of ca. 300 Ka can be estimated for the base of this upper unit, considering mean accumulation rates of 10 cm/Kyr that characterize alluvial sedimentation for the rest of the Lebrija Formation. In this case, the temporal gap between the two units of the Lebrija Formation must represent around 1.3 Myr (Fig. 7). With regards to the Almonte Formation, and keeping in mind that this is a lateral equivalent of the Lebrija Formation, variable mean accumulation rates between about 1 and 6 cm/Kyr can be established for this formation.

Concerning the Huelva Formation, no magnetostratigraphic data are available in the LE borehole. Thus, the age of neither its different stratigraphic intervals, nor its base, can be magnetostratigraphically constrained. Nevertheless, the base of the Huelva Formation broadly coincides with the Miocene/Pliocene boundary (Sierro et al., 1996; González-Delgado et al., 2004) dated at 5332 Ma (Lourens et al., 2004; Gradstein et al., 2004). The top of the Huelva Formation lies in the uppermost part of chron C2Ar, and therefore is ~3.7 Ma near the end of the Early Pliocene (Fig. 8). Taking into consideration that the base of the Huelva Formation was not reached in LE borehole at –336 m, a minimum mean accumulation rate of 7 cm/Kyr can be estimated for this formation at LE borehole.

5.2. Correlation with the surrounding northern areas

Based on the results shown above, we provide new insight on the correlation of the Late Pliocene to Holocene sediments between the Guadalquivir marshlands and those deposited in the northern areas of the lower Guadalquivir basin. To the south and east, the lack of subsoil data prevents the establishment of a reliable correlation.

5.2.1. Correlation with the Aljarafe high and the Almonte plain

The Aljarafe is a topographic high area located north of the marshlands, between the Guadiamar and Guadalquivir rivers (Figs. 1 and 8 cross-section A). It constitutes a monocline gently dipping to the south, made up of an up to 30 m-thick sequence of yellowish sands and sandstones. Toward the south, the Aljarafe sands grade laterally to the Huelva Formation, which is buried within the marshlands, beneath the Almonte, Lebrija and Marismas formations. In the southern part of the high, the Aljarafe sands are overlain by a 25 m-thick sequence of red coarse-grained clastic sediments of alluvial origin (the Red Formation of Torres et al., 1977b). These sediments are well exposed in several old quarries along the southern edge of the Aljarafe high. In these quarries well rounded alluvial gravels with coarse pebbles of up to 25 cm in size are shown, in layers that have common paleochannel and cross-bedding structures. Clasts display the same metamorphic and igneous composition as in the Almonte Formation. The sedimentological features of these sediments, coupled with borehole data, indicate that the Red Formation is a lateral equivalent of the Almonte Formation, bellow the Marismas and the upper unit of the Lebrija Formation.

The gentle southward-dipping monocline of the Aljarafe extends further west into the Almonte plain (Figs. 1 and 8 cross-section B). In that area, a 20 m-thick sequence of variegated sands and gravels (the Bonares Formation of Mayoral and Pendón, 1986–87) crops out overlying the Huelva Formation. On the basis of the stratigraphic position of the Bonares Formation, equivalent to Aljarafe sands, this formation is interpreted to constitute a lateral equivalent of the uppermost part of the Huelva Formation. Based on our results, an Early Pliocene age can be inferred for the Aljarafe and the Bonares formations. In the Almonte plain, the lateral equivalent of the Almonte Formation is the High Alluvial Level of Pendón and Rodríguez-Vidal (1986-87). It is mainly represented in the outcrops of the westernmost part of the basin (Fig. 1), where it cuts the Huelva and Bonares formations. The boundary is indeed an erosive surface

The Red Formation and the High Alluvial Level constitute the proximal sediments of the alluvial system that originates the Almonte Formation. Rodríguez-Vidal (1989) interprets such proximal sediments as the ones originated by braided rivers coming from the Sierra Morena, which is consistent with the inferred interpretation for the Almonte Formation.

5.2.2. Correlation with the alluvial terraces of the Guadiamar River

The Guadiamar River is a N-S flowing river that drains the Sierra Morena and the northern part of the lower Guadalquivir basin, where respectively it cuts Paleozoic rocks and Neogene sediments of the Gibraleón and Aljarafe formations before flowing into the Guadalquivir marshlands (Fig. 1). Apart from the present-day alluvial plain (labelled T0), this river developed a system of three terraces labelled T1 to T3 (Salvany, 2004) (Fig. 9). According to radiocarbon dating, T1 and the uppermost part of T2 are Holocene in age. In the lower part of T2, the age is beyond the range of radiocarbon dating (Salvany et al., 2004). Radiocarbon data suggest that T2 correlates with the prominent package of gravels and sands intercalated within the middle part of the Marismas Formation at LE borehole, between 48 and 56 mbs, which also ranges between Late Pleistocene and Holocene in age (Fig. 9). In the upper part of the Guadiamar valley T3 is located about 25 m above T1 and T2. This height gradually decreases toward the valley mouth where T3 descends below the younger terraces. In the marshlands area, borehole and chronologic data suggest that T3 is a lateral equivalent of the upper unit of the Lebrija Formation, which is consistent with an inferred Middle Pleistocene age for both units (Fig. 9).

5.3. Tectono-sedimentary evolution

As a whole, the continental Plio-Quaternary sediments of the lower Guadalquivir basin form a wedge-shaped deposit that thickens towards the Betic thrust front of the basin (Fig. 8). The deposit has a basal unconformity overlain by coarse gravels that pass upwards to gravel-bearing clays and then to clays and sands in the upper part. This deposit forms a fining and thinning-upward sequence that can be considered a second-order sequence in the context of the whole infill of the basin. In turn, this sequence consists of three sequences of minor (third) order, each one showing a stratigraphic trend similar to main one (Fig. 10).

Sequence 1 is the lowest and thickest one. It is composed of proximal-alluvial sediments of the Almonte Formation and of distal-alluvial sediments of the lower unit of the Lebrija Formation. Sequence 2 has an intermediate thickness, comprising the proximal-alluvial sediments of the upper unit of the Lebrija Formation and the distal-alluvial sediments of the lower part of the Marismas Formation. Sequence 3, the uppermost and thinnest one, is composed of distal-alluvial, estuarine and marsh sediments of the upper part of the Marismas Formation. The chronostratigraphic data allow dating these sequences respectively as late Pliocene to early Plesitocene (3.7–1.6 Ma), early to late Pleistocene (1.6–0.015 Ma), and latest Pleistocene to present-day (15–0 Ka).

Sequence 1 represents the onset of continental sedimentation in the lower Guadalquivir basin (Fig. 10–1). Its basal erosive surface indicates that an important downcutting period preceded the accumulation of continental sediments. At that time, braided rivers sourced in the Sierra Morena transported coarse clastics throughout the basin, including well beyond the present coastline of the Gulf of Cádiz. Subsequent subsidence of the basin concurred with a retrogradation of the alluvial system, so that the braided rivers that initially spread throughout most of the basin gradually retreated towards the source area.

This sedimentary evolution can be explained in light of the tectonic scenario envisaged for the Guadalquivir basin by García-Castellanos et al. (2002) on the basis of geophysical data and modelling. According to these authors, a substantial part of the present relief of Sierra Morena is related to its uplift as a forebulge of the Betic Cordillera. During the syn-orogenic period (late Serravallian to Tortonian) the Betic thrust wedge loading caused a flexural forebulge in the craton margin of the basin that was onlaped and buried by contemporary marine sediments. Once thrusting ended (post-orogenic period), the viscous relaxation of the lithosphere developed an emergent forebulge migrating southward, narrowing the basin and uplifting its distal sediments. This post-orogenic period started at around 6.5 Ma (early Messinian) and extended throughout the latest Miocene, Pliocene and Quaternary (Berástegi et al. 1998). In the LE borehole, is around 3.7 Ma (Early-Late Pliocene boundary) the first clear evidence of this forebulge uplift. Continued northward retrogradation of the alluvial system between 3.7 and 1.6 Ma likely reflected the progressive denudation of forebulge of the Sierra Morena during a subsequent quiescent phase.

The development of flexural forebulges is a common feature of many foreland basin systems (DeCelles and Giles, 1996; Catuneanu, 2004). In general, it is stated that forebulge uplift occur coeval to foredeep subsidence, both related to thrust loading of an orogenic belt (Beaumont et al., 1988). During an overthrust phase the immediate response of the lithosphere to loading is elastic and results in a downwarped flexural basin adjacent to the orogen and the elevation of a peripheral forebulge along the cratonward edge of the basin. If the thrust load remains unchanged for a long period, viscous relaxation of the plate-bending stress results in deepening of the basin, as well as uplift of the forebulge and its contraction toward the load (Quinlan and Beaumont, 1984; Tankard, 1986; Sinclair et al., 1991).

Sequence 2 is preceded by a new period of downcutting between 1.6–0.3 Ma, which affected the whole basin and likely resulted in the by-pass of sediments towards the present-day offshore of the Gulf of Cádiz. This erosive event is linked to a new period of forebulge rebound of the Sierra Morena, developed together with a significant migration of the forebulge into the basin. This reflects the viscous relaxation phase envisaged in the model of Garcia-Castellanos et al. (2002) (Fig. 10–2). Hereby, the hinge line that delimits forebulge and foredeep shifted toward the SSE at least 40 km. This line became a tilt axis from which the marshlands area sank as the northern part of the basin uplifted.

The uplift of the northern part of the basin triggered the reworking of continental sediments accumulated in the previous sequence (i. e., the High Alluvial Level and the

Red Formation), which then started to develop as a denudation plain gently dipping towards the SSE. The Neogene deposits of the northern part of the basin were exhumed and also reworked into the basin. After de erosion, a relatively sudden spread of alluvial sediments developed throughout the northern part of the marshlands area. Alluvial sediments of the upper unit of the Lebrija Formation were supplied by the early Guadiamar River, which, at the same time, developed terrace T3, as well as by its contemporary Guadalquivir River. The distal part of the alluvial system gave way to the lowermost sediments of the Marismas Formation, which gradually expanded northward over the proximal alluvial sediments. This system was bounded to the east by the Abalario sands, which prograded south-eastward starting early in the first sequence.

The third sequence is characterized by the development of terrace T2 in the Guadiamar valley. The development of this terrace was preceded by a third period of dawn-cutting, which left remains of terrace T3 on the surrounding hills. Beyond the Guadiamar valley, the erosion was restricted to the easternmost part of the marshlands, where some alluvial channels were excavated through the uppermost sediments of the preceding sequence (Fig. 10-3). This sequence would represent a last smaller pulse of the Sierra Morena.

Since 6 Ka, this uppermost sequence witnessed a marked transgression so that marine restricted facies (i. e., the upper part of the Marismas Formation) accumulated in an estuary that was bounded by tidal flats and minor distal alluvial plains near the mouth of the Guadiamar River, which then developed terrace T1, and the Gualdalquivir River (Fig. 10–4). In historical times, the SSE progradation of the Doñana spitbar in the south-easternmost tip of the Abalario led to the closure of the estuary to the open sea, giving way to the present-day marshland environment (Rodríguez-Ramírez, 1998). The last 300 years have witnessed a last incision of the fluvial network, resulting in the formation of terrace T0 along the Guadiamar valley (Salvany, 2004) and in the development of small deltas built by the main streams flowing into the marshlands (Bayán and Dolz, 1995).

The influence of forebulge dynamics in basin infilling are documented in many studies (Heller et al., 1988; Fleming and Jordan, 1990; Sinclair et al., 1991; Plint et al. 1993; Crampton and Allen, 1995; Catuneanu and Sweet, 1999). In general, as occurred in the study case and agreeing with our interpretation, these studies demonstrate that each phase of forebulge uplift leads to an unconformity on its flanks and the shift of the sedimentary facies. Subsequent denudation of the emerged forebulge normally supplies the basin with clastic sediment with the main sedimentary infill coming from denudation of the thrust area (Heller et al., 1988; Fleming and Jordan, 1990; Plint et al., 1993). In the study case, the lithology of the pebbles and sand shows that they dominantly were supplied from the craton margin of the basin. The apparent lack of sediments coming from the thrust area is difficult to understand, and is not resolved in our study. Probably, the present-day marshlands represent only a small part of the Plio-Quaternary foredeep, whose proximal part remains partially hidden below more recent thrust-sheets where subsoil data are unavailable.

The explained tectono-sedimentary evolution of the lower Guadalquivir basin suggests a late Pliocene to Quaternary decreasing uplift of the Sierra Morena forebulge, related to a coeval decrease of the contractional deformation of the Betic orogen. This contractional deformation would be generated by a NNW-SSE compression that persisted along this period, which is consistent with the regional tectonic studies that deal with the Betic Cordillera and related Guadalquivir foreland basin (Galindo-Zaldívar et al., 1993; Morales et al., 1999).

6. Conclusions

This study dates the onset of continental sedimentation in the lower Guadalquivir basin at the Early Pliocene-Late Pliocene boundary as 3.7 Ma in the LE borehole. Since then, the basin has mainly filled by alluvial sediments of the Almonte and Lebrija formations and the lower part of the Marismas Formation, as well as by aeolian and shallow marine sediments of respectively the Abalario Formation and the upper part of the Marismas Formation. These formations form three fining-upward depositional sequences that attest to the uplift of the craton side of the basin (i. e., the Sierra Morena) as a forebulge of the Betic Cordillera and to the simultaneous greatest subsidence of the basin along to the Betic deformation front. From radiocarbon and magnetostraigraphic data, these sequences are dated Late Pliocene to Early Pleistocene (3.7–1.6 Ma), Early to Late Pleistocene (1.6–0.015 Ma), and latest Pleistocene to present-day (15–0 Ka).

Each sequence is characterized by: first, an initial period of down-cutting that produced a regional unconformity; second, a rapid alluvial progradation supplied by the craton margin of the basin along the thrust front; and third, a slow alluvial retrogradation cratonward. In the third sequence, retrogradation occurred together with a shallow marine transgression that flooded the southern part of the basin. The rapid alluvial progradation of the first and second sequences attest to two main periods of increased forebulge uplift at 3.7 Ma and 1.6-0.3 Ma. A period of minor uplift at the Pleistocene-Holocene boundary is represented by the basal erosion of the third sequence. The subsequent episodes of slower alluvial retrogradation reflect decreased forebulge uplift and its denudation.

In most foreland basins, the facies architecture and sediment supply are largely controlled by the adjacent orogenic belt some distance from the craton. In contrast, the late evolution of the lower Guadalquivir basin at least since Late Pliocene was mainly controlled by tectonic uplift and sediment supply from the craton side (Sierra Morena).

AKNOWLEDGEMENTS

This study was developed by the IGME (Instituto Geológico y Minero de España, in Sevilla) in collaboration with the UPC (Universitat Politècnica de Catalunya, in Barcelona) and the IJA (Institut de Ciències de la Terra Jaume Almera, in Barcelona), between 2004 and 2008 in the framework of a research project focused on the stratigraphy and sedimentology of the Neogene and Quaternary deposits of the lower Guadalquivir basin. The authors wish to thank Drs. Emilio Custodio (UPC) and Vicente Gabaldón (IGME) for promoting this project and helping its development, and Drs. Jesús Galindo-Zaldíbar (Universidad de Granada) and Oriol Oms (Universitat Autònoma de Barcelona) for their critical reading of the first version of the manuscript. The authors also acknowledge Dr. A.D. Miall and other two anonymous reviewers, and the Editor, Dr. Brian Jones, for their comments, which greatly improve the manuscript.

REFERENCES

Armijo, R., Benkhelil, J., Bousquet, J.Cl., Estévez, A., Guiraud, R., Montenat, Ch., Pavillon, M.J., Philip, H., Sanz de Galdeano, C., Viguier, CL., 1977. Chapitre III, Les résultats de l'analyse structurale en Espagne. In: Grupe de recherche néotectonique de l'Arc de Gibraltar. L'histoire tectonique récent (Tortonien à Quaternaire) de l'Arc de Gibraltar et des bordures de la mer d'Alboran. Bull. Soc. Geol. France 7–19, 575–614.

Baceta, J.I., Pendón, J.G., 1999. Estratigrafía y arquitectura de facies de la Formación Niebla, Neógeno Superior, sector occidental de la cuenca del Guadalquivir. Rev. Soc. Geol. España 12, 419–438.

Bayán, B., Dolz, J., 1995. Las aguas superficiales y la marisma del Parque Nacional de Doñana. Revista de Obras Públicas 3340, 17–29.

Beaumont, Ch., Quinlan, G., Hamilton, J., 1988. Orogeny and stratigraphy: numerical models of the Paleozoic in the Eastern Interior of North America. Tectonics 7-3, 389-416.

Berastegui, X., Banks, C.J., Puig, C., Taberner, C., Waltham, D., Fernández, M., 1998. Later diapiric emplacement of Triassic evaporites at the southern margin of the Guadalquivir Basin, Spain. In: Mascle, A., Puigdefàbregas, C., Luterbacker, H.P., Fernández, M. (Eds.), Cenozoic Foreland Basins of Western Europe. Geological Society Special Publication 134, 49–68.

Borja, F., Díaz del Olmo, F., 1992. Eastern sector of the cliff at El Asperillo (Huelva coast, SW Spain): formation and chronology. MBSS Newsletter 14, 87–93.

Caratini, C., Viguier, C., 1973. Étude palynologique et sédimentologique des sables hologenes de la falaise littorale d'El Asperillo (province de Huelva). Estudios Geológicos 29, 325–328.

Carretero, M.I., Ruiz, F., Rodríguez-Ramírez, A., Cáceres, L., Rodríguez-Vidal, J., González-Regalado, M.L., 2002. The use of clay minerals and microfossils in palaeoenvironmental reconstruction: the Holocene littoral strand of Las Nuevas (Doñana Nacional Park) SW Spain. Clay Minerals 37, 93–103.

Catuneanu, O., 2004. Retroarc foreland systems evolution through time. Journal African Earth Sciences 38, 225-242.

Catuneanu, O., Sweet, A.R., 1999. Maastrichtian-Paleocene forland-basin stratigraphies, western Canada: a reciprocal sequence architecture. Can. J. Earth Sci. 36, 685-703.

Civis, J., Sierro, F.J., González-Delgado, J.A., Flores, J.A., Andrés, I., Porta, J., Valle, M.F., 1987. El Neógeno marino de la provincia de Huelva: antecendentes y definición de las unidades litoestratigráficas. Stud. Geol. Salmantina, special issue, pp 9–21.

Civis, J., Dabrio, C.J., González-Delgado, J.A., Goy, J.L., Ledesma, S., Pais, J., Sierro, F.J., Zazo, C., 2004. Cuenca del Guadalquivir. In: Vera, J.A. (Ed.), Geología de España. Madrid, SGE-IGME, pp 543–550.

Crampton, S.L., Allen, P.A., 1995. Recognition of forebulge unconformities associated with early stage foreland basin development: example from the North Alpine Foreland Basin. AAPG Bull. 79-10, 1495-1514.

Cruse, K., 1979. A review of water well drilling methods. Quarterly Journal of Engineering Geology 12, 79–95.

Dabrio, C.J., Borja, F., Zazo, C., Boersma, J.R., Lario, J., Goy, J.L., Polo, M.D., 1996. Dunas eólicas y facies asociadas pleistocenas y holocenas en el acantilado del Asperillo (Huelva). Geogaceta 20, 1089–1092.

De Celles, P.G., Giles, K.A., 1996. Foreland basin systems. Basin Research 8, 105-123.

FAO (1970) Estudio hidrogeológico de la Cuenca del Guadalquivir: informe técnico. 1 AGL: SF/SPA 9, Roma, unpublished report, pp 1-115.

Fernández, M., Berastegui, X., Puig, C., García-Castellanos, D., Jurado, M.J., Torné, M., Banks, C., 1998. Geophysical and geological constraints on the evolution of the Guadalquivir foreland basin, Spain. In: Mascle, A., Puigdefàbregas, C., Luterbacker, H.P., Fernández, M. (Eds.), Cenozoic Foreland Basins of Western Europe. Geological Society Special Publication 134, pp 29–48.

Fleming, P.B., Jordan, T.E., 1990. Stratigraphic modelling of foreland basins: interpreting thrust deformation and lithosphere rheology. Geology 18, 430-434.

Flor, G., 1990. Tipología de dunas eólicas. Procesos de erosió-sedimentación costera y evolución litoral de la provincia de Huelva (Golfo de Cádiz occidental, Sur de España). Estudios Geológicos 46, 99–109.

Flores-Hurtado, E., Rodríguez-Vidal, J., 1994. Rasgos morfotectónicos del interfluvio costero Guadiana-Guadalquivir (Golfo de Cádiz). In: Arnáez, J., García-Ruiz, J.M., Gómez-Villar, A. (Eds.), Geomorfología en España. Sociedad Española de Geomorfología. Logroño, pp 13–19.

Galindo-Zaldívar, J., González-Lodeiro, F., Jabaloy, A., 1993. Stress and palaeostress in the Betic-Rif cordillera (Miocene to the present). Tectonophysics 227, 105-126.

García-Castellanos, D., Fernández, M., Torné, M., 2002. Modeling the evolution of the Guadalquivir foreland basin (southern Spain). Tectonics 21, 1–17.

Gibbard, Ph.L., Head, M.J., Walker, M.J.C., Subcommission on Quaternary Stratigraphy, 2009. Formal ratification of the Quaternary System/Period and the Pleistocene Series/Epoch with a base at 2.58 Ma. Journal of Quaternary Science 25, 96-102.

González-Delgado, J.A., Civis, J., Dabrio, C.J., Goy, J.L., Ledesma, S., Pais, J., Sierro, F.J., Zazo, C., 2004. Cuenca del Guadalquivir. In: Vera, J.A. (Ed.), Geología de España. Madrid, SGE-IGME, pp 543–550.

Goy, J.L., Zazo, C., Dabrio, C.J., Lario, J., 1994. Fault controlled shifting shorelines in the Gulf of Cadiz since 20ky BP. 1º Simpósio sobre a margem continental ibérica atlântica, Lisboa. Abstracts, 24.

Goy, J.L., Zazo, C., Dabrio, C.J., Lario, J., Borja, F., Sierro, F., Flores, J.A., 1996. Global and regional factors controlling changes of coastlines in southern Iberia (Spain) during the Holocene. Quaternary Science Reviews 15, 773–780.

Gradstein, F.M., Ogg, J.G., Smith, A.G., Bleeker, W., Lourens, L.J., 2004. A new geological time scale, with special reference to Precambrian and Neogene. Episodes 27, 83–100.

Heller, P.L., Angevine, Ch.L., Winslow, N.S., Paola, Ch., 1988. Two-phase stratigraphic model of foreland-basin sequences. Geology 16, 501-504.

IGME, 1983. Hidrogeología del Parque Nacional de Doñana y su entorno. Servicio de Publicaciones del Ministerio de Industria y Energía, Madrid. pp 1-120.

IRYDA, 1976. Informe final de los sondeos de la zona regable de Almonte-Marismas (Huelva-Sevilla). Unpublished report, pp 1-100.

Kirschvink, J.L., 1980. The least-squares line and plane and the analysis of paleomagnetic data, Geophys. J. R. Astron. Soc. 62, 699–718.

Lario, J., Zazo, C., Plater, A.J., Goy, J.L., Dabrio, C.J., Borja, F., Sierro, F.J., Luque, L., 2001. Particle size and magnetic propierties of Holocene estuarine deposits from the Doñana National Park (SW Iberia): evidence of gradual and abrupt coastal sedimentation. Z. Geomorph. N. F. 45, 33–54

Lario, J., Zazo, C., Goy, J.L., Dabrio, C.J., Borja, F., Silva, P.G., Sierro, F., González, A., Soler, V., Yll, E., 2002. Changes in sedimentation trends in SW Iberia Holocene estuaries (Spain). Quaternary International 93–94, 171–176.

Leyva, F., Pastor, F., 1976. Mapa Geológico de España 1:50.000, 1017, El Abalario. IGME, Servicio de Publicaciones del Ministerio de Industria, Madrid.

Lourens, L.J., Hilgen, F.J., Shackleton, N.J., Laskar, J., Wilson, D.S., 2004. The Neogene period. In: Gradstein, F.N., Ogg, J.G., Smith, A.G. (Eds.), A Geologic Time Scale 2004. Cambridge University Press, pp 409–440.

Magne, J. and Viguier, Cl. (1974) Stratigraphie du Néogène marin “post-nappe” de l’Andalousie occdentale. *Mem. B.R.G.M.*, 78–2, 821–827.

Martínez del Olmo, W., García-Mojonero, C., Torrescusa, S., 2005. The Guadalquivir and Gulf of Cádiz gas basins (SW, Spain). Publ. Asociación de Geólogos y Geofísicos Españoles del Petroleo, 25 aniversario, 105–121.

Mayoral, E., Pendón J.G., 1986–87. Icnofacies y sedimentación en zona costera. Plioceno superior (?), litoral de Huelva. Acta Geológica Hispánica 21–22, 507–513.

Menanteau, L., 1979. Les marismas du Guadalquivir. Example de transformation d’un paisaje alluvial au cours du Quaternaire récent. Ph D Thesis, Université Paris-Sorbone, pp 1-154.

Morales, J., Serrano, I., Jabaloy, A., Galindo-Zaldívar, J., Zhao, D., Torcal, F., Vidal, F., González-Lodeiro, F., 1999. Active continental subduction beneath the Betic Cordillera and the Alboran Sea. Geology 27, 735-738.

Pendón, J.G., Rodríguez-Vidal, J., 1986–87. Caracteres sedimentológicos y geomorfológicos del Alto Nivel Aluvial cuaternario en el litoral de Huelva. Acta Geológica Hispánica 21–22, 107–111.

Perconig, E., Martínez-Díaz, C., 1977. Perspectivas petrolíferas de Andalucía Occidental. Boletín Geológico y Minero 88, 417–433.

Plint, A.G., Hart, B.S., Donaldson, W.S., 1993. Lithospheric flexure as a control on stratal geometry and facies distribution in Upper Cretaceous rocks of the Alberta foreland basin. Basin Research 5, 69-77.

Pozo, M., Carretero, M.I., Ruiz, F., Rodríguez-Vidal, J., Cáceres, L.M., Abad, M., 2008. Caracterización mineralógica de facies sedimentarias de edad Pleistoceno superior-Holoceno en el Parque Nacional de Doñana (Huelva). Implicaciones paleoambientales. Geo-Temas 10, 953–956.

Pozo, M., Ruiz, F., Carretero, M.I., Rodríguez-Vidal, J., Cáceres, L.M., Abad, M., González-Regalado, M.L., 2010. Mineralogical assemblages, geochemistry and fossil associations of Pleistocene-Holocene complex siliciclastic deposits from the Southwestern Doñana National Park (SW Spain): A palaeoenvironmental approach. Sedimentary Geology 225, 1-18.

Quinlan, G.M., Beaumont, Ch., 1984. Appalachian thrusting, lithosphere flexure, and the Paleozoic stratigraphy of the Eastern Interior of North America. Can. J. Earth Sci. 21, 973-996.

Rodríguez-Ramírez, A., 1998. *Geomorfología del Parque Nacional de Doñana y su entorno*. Publ. Ministerio de Medio Ambiente, Organismo Autónomo Parques Nacionales, pp 1-146.

Rodríguez-Ramírez, A., Rodríguez-Vidal, J., Cáceres, L.M., Clemente, L., Belluomini, G., Manfra, L., Improta, S., de Andrés, J.R., 1996a. Evolución costera de la desembocadura del Guadalquivir en los últimos 6000 años (SW de España). Geogaceta 20, 1086–1088.

Rodríguez-Ramírez, A., Rodríguez-Vidal, J., Cáceres, L., Clemente, L., Belluomini, G., Manfra, L., Improta, S., de Andrés, J.R., 1996b. Recent coastal evolution of the Doñana Nacional Park (SW Spain). Quaternary Science Reviews 15, 803–809.

Rodríguez-Ramírez, A., Cáceres, L.M., Ruiz, F., González-Regalado, M.L., Muñiz, F., Rodríguez-Vidal, J., Abad, M., Carretero, M.I., 2001. Génesis y caracterización del cordón estuarino de Las Nuevas (P.N. de Doñana). Geogaceta 29, 103–106.

Rodríguez-Vidal, J. (1989) El inicio de la red fluvial cuaternaria en el sector occidental de la Depresión del Guadalquivir. In: *El Cuaternario en Andalucía Occidental* (Ed. by F. Díaz del Olmo and J. Rodríguez Vidal). AEQUA Monografías, 1, 27–31.

Ruiz-Muñoz, F., González-Regalado-Montero, M.L., Redondo-Sanz, J.L., 1997. Guía de fósiles del sur de la provincia de Huelva. Diputación de Huelva, pp 1-205.

Ruiz, F., Rodríguez-Ramírez, A., Cáceres, L.M., Rodríguez-VidaL, J., Carretero, M.I., Clemente, L., Muñoz, J.M., Yañez, C., Abad, M., 2004. Late Holocene evolution of the Southwestern Doñana National Park (Guadalquivir Estuary, SW Spain): a multivariable approach. Palaeogeogr, Palaeoclimatol, Palaeoecol 204, 47–64.

Ruiz, F., Rodríguez-Ramírez, A., Cáceres, L.M., Rodríguez-Vidal, J., Carretero, M.I., Abad, M., Olias, M., Pozo, M., 2005. Evidence of high-energy events in the geological record: Mid-holocene evolution of the Southwestern Doñana National Park (SW Spain). Palaeogeogr, Palaeoclimatol, Palaeoecol 229, 212–229.

Salvany, J.M., 2004. Tilting neotectonics of the Guadiamar drainage basin, SW Spain. Earth Surface Processes and Landforms 29, 145–160.

Salvany, J.M., Custodio, E., 1995. Características litoestratigráficas de los depósitos plio-cuaternarios del bajo Guadalquivir en el área de Doñana: implicaciones hidrogeológicas. Rev. Soc. Geol. de España 8, 21–31.

Salvany, J.M., Carrera, J., Bolzicco, J., Mediavilla, C., 2004. Pitfalls in the geological characterization of alluvial deposits: site investigation for reactive barrier installation at Aznalcóllar, Spain. Quarterly Journal of Engineering Geology and Hydrogeology 37, 141–154.

Sanz de Galdeano, C., Vera, J.A., 1992. Stratigraphic record and palaeogeographical context of the Neogene basins in the Betic Cordillera, Spain. Basin Research 4, 21-36.

Sierro, F.J. (1985) Estudio de los foraminíferos plantónicos, bioestratigrafía y cronoestratigrafía del Mio-Plioceno del borde occidental de la Cuenca del Guadalquivir (SO de España). *Studia Geologica Salmanticensia*, 21, 7–85.

Sierro, F.J., González-Delgado, J.A., Dabrio, C.J., Flores, J.A., Civis J., 1996. Late Neogene depositional sequences in the foreland basin of Guadalquivir (SW Spain). In: Friend, P.F., C.J. Dabrio, C.J. (Eds.), Tertiary basins of Spain, the stratigraphic record of crustal kinematics. World and Regional Geology 6. Cambridge University Press, pp 339–345.

Sinclair, H.D., Coakley, B.J., Allen, P.A., Watt, A.B., 1991. Simulation of foreland basin stratigraphy using a diffusion model of mountain belt uplift and erosion: an example from the Central Alps, Switzerland. Tectonics 10-3, 599-620.

Tankard, A.J., 1986. Depositional response to foreland deformation in the Carboniferous of Eastern Kentucky. *AAPG Bull.* 70-7: 853-868.

Torres-Perezhidalgo, T., Fernández-Luanco, M.C., Leyva-Cabello, F., Granados, L.F., Martínez-Fresneda, F., Pan-Arana, T., Antón-Alfonso, S., 1977a. Mapa Geológico de España 1:50.000, hoja 1001, Almonte. IGME, Servicio de Publicaciones del Ministerio de Industria, Madrid.

Torres-Perezhidalgo, T., Fernández-Luanco, M.C., Leyva-Cabello, F., Granados, L.F., Martínez-Fresneda, F., Borragán-Pastor, J., Antón-Alfonso, S., 1977b. Mapa Geológico de España 1:50.000, hoja 1002, Dos Hermanas. IGME, Servicio de Publicaciones del Ministerio de Industria, Madrid.

Viguier, C., 1977. Les grands traits de la tectonique du basin néogène du Bas Guadalquivir. Boletín Geológico Minero 88, 39–44.

Zazo, C., Goy, J.L., Somoza, L., Dabrio, C.J., Belluomini, G., Improta, S., Lario, J., Bardají, T., Silva, P.G., 1994. Holocene sequence of sea-level fluctuations in relation to climatic trends in the Atlantic-Mediterranean linkage coast. Journal of Coastal Research 10, 933–945.

Zazo, C., Dabrio, C.J., González, A., Sierro, F., Yll, E.I., Goy, J.L., Luque, L., Pantaleón-Cano, J., Soler, V., Roure, J., Lario, J., Hoyos, M., Borja, F., 1999a. The record of the latter glacial and interglacial periods in the Guadalquivir marshlands (Mari López drilling, SW Spain). Geogaceta 26, 119–122.

Zazo, C., Dabrio, C.J., Borja, J.L., Lezine, A.M., Lario, J., Polo, M.D., Hoyos, M., Boersma, J.R., 1999b. Pleistocene and Holocene aeolian facies along the Huelva coast (sothern Spain): climatic and neotectonic implications. Geologie en Mijnbouw 77, 209–224.

Zazo, C., Mercier, N., Silva, P.G., Dabrio, C.J., Goy, J.L., Roquero, E., Soler, V., Borja, F., Lario, J., Polo, D., de Luque, L., 2005. Landscape evolution and geodynamic control in the Gulf of Cadiz (Huelva coast, SW Spain) during the Late Quaternary. Geomorphology 68, 269–290.

Zazo, C., Dabrio, C.J., Goy, J.L., Lario, J., Cabero, A., Silva, P.G., Bardají, T., Mercier, N., Borja, F., Roquero, E., 2008. The coastal archives of the last 15ka in the Atlantic-Mediterranean Spanish linkage area: Sea level and climatic changes. Quaternary International 181, 72–87.

Zijderveld, J.D.A., 1967. Demagnetization of rocks: analysis of results. In: Collinson D.W., Creer, K.M., Runcorn, S.K. (Eds.), Methods in Palaeomagnetism. Elsevier, Amsterdam, pp 254–286.

FIGURE CAPTIONS

Table 1. Study boreholes drilled by IGME in the Abalario high and Guadalquivir marshlands of the lower Guadalquivir basin.

Table 2. Radiocarbon ages of samples from the studied boreholes in the Guadalquivir marshlands.

Figure 1. Geological map of the lower Guadalquivir basin, and location of study boreholes and cross-sections in figures 2, 3, 4 and 5 (map adapted from IGME's 1:50.000 geological maps).

Figure 2. Lithologic logs and correlation of study boreholes in cross-sections 1 and 2. See Figure 1 for locations.

Figure 3. Lithologic logs and correlation of study boreholes in cross-sections 3 and 4. See Figure 1 for locations and Figure 2 for legend.

Figure 4. Lithologic logs and correlation of study boreholes in cross-section 5. See Figure 1 for locations and Figure 2 for legend.

Figure 5. Lithostratigraphic cross-sections of the Plio-Quaternary formations through the Abalario and the Guadalquivir marshlands as derived from the study boreholes described in Figures 2, 3 and 4. See Figure 1 for locations.

Figure 6. Demagnetization plots representative of the different formations studied. Grey lines represent the linear fit to calculated ChRM directions. Demagnetization plots are in geographic coordinates with arbitrary cardinal points, and temperature steps are in ºC. The quality of ChRM directions is indicated. Dark lines indicate the fit to the ChRM directions. Solid (open) circles represent projections in the horizontal (vertical) plane.

Figure 7. Sequence of polarity changes established for Lebrija borehole and its correlation to the ATNTS2004 (Lourens et al., 2004; Gradstein et al., 2004). The age of the Pliocene-Pleistocene boundary is updated according to Gibbard et al. (2009). Mean accumulation rates between main reversals (black dots) are given in cm/Kyr. The undulated line indicates the position of a sedimentary gap or hiatus. The upper arrow indicates the position of the oldest sample with an age that is within the range of radiocarbon dating, and the lower one indicates the position of a sample with an age that is beyond that range. The estimated ages for the base of the Lebrija Formation (3.7 Ma), the long hiatus (1.6-0.3 Ma), the base of the Marismas Formation (85-110 ka), and the position of the Pleistocene-Holocene boundary (11.5 ka) have been indicated using bold labels.

Figure 8. Lithostratigraphic cross-sections through four areas of the lower Guadalquivir basin, based on the correlation of representative hydrogeologic boreholes (vertical lines) drilled in the region.

Figure 9. Correlation between the Guadiamar alluvial terraces and the LE borehole of the Guadalquivir marshlands. Upper part: longitudinal cross-section from the Guadiamar Valley to the LE borehole, adapted from Salvany (2004). Lower part: schematic cross-section (without scale) of the Guadiamar alluvial terraces representative of the northern half of the valley, and radiocarbon ages from Salvany (2004) and Salvany et al. (2004)

Figure 10. Schematic cross-sections (without scale) and paleogeographic maps illustrating the sedimentary evolution of the lower Guadalquivir basin during the Upper Pliocene and Quaternary.

Chronology and tectono-sedimentary evolution of the Late Pliocene to Quaternary deposits of the lower Guadalquivir foreland basin, SW Spain

Josep Maria Salvany [1], Juan Cruz Larrasoaña [2], Carlos Mediavilla [3], Ana Rebollo [3]

[1] Dept. Enginyeria del Terreny, Universitat Politècnica de Catalunya, c/ Gran Capità s/n, D2, 08034 Barcelona (Spain). E-mail: josepm.salvany@upc.edu

[2] Institut de Ciències de la Terra “Jaume Almera”, CSIC, c/ Solé i Sabarís s/n, 08028 Barcelona (Spain). Now at: Area de Cambio Global, Instituto Geológico y Minero de España, Oficina de Proyectos de Zaragoza, C/ Manuel Lasala 44, 9B, 50006 Zaragoza (Spain)

[3] Instituto Geológico y Minero de España, Plaza de España, Torre Norte, 41013 Sevilla (Spain)

Correspondance addressed to JM Salvany

ABSTRACT

This paper presents new litho, chrono and magnetostratigraphic data from cores of 23 exploratory boreholes drilled in the Abalario and marshlands areas of the lower Guadalquivir basin (the western sector of the Guadalquivir foreland basin, SW of Spain). The lithologic logs of these boreholes identify four main sedimentary formations, namely: Almonte Sands and Gravels, Lebrija Clays and Gravels, Marismas Clays and Abalario Sands, respectively interpreted as proximal-alluvial, distal-alluvial, alluvial-estuarine and aeolian. From radiocarbon and magnetostratigraphic data, these formations were dated as Late Pliocene to Holocene. In the marshlands area, three main sedimentary sequences are present: a Late Pliocene-Early Pleistocene sequence of the Almonte and Lebrija (lower unit) formations, a Late Pleistocene-Early Holocene sequence of the Lebrija (upper unit) and Marismas formations, and a middle Holocene to present-day sequence of the upper Marismas Formation. The three sequences began as a rapid alluvial progradation on a previously eroded surface, and a subsequent alluvial retrogradation. In the third sequence, shallow estuarine and marsh sediments accumulated on top of the alluvial sediments. The aeolian sands of the Abalario topographic high developed coeval to alluvial and estuarine sedimentation after the first alluvial progradation, and continuously until the present. Correlation with the surrounding areas show that the sequences are the result of the forebulge uplift of the northern margin of the basin (Sierra Morena) and the adjacent Neogene oldest sediments of their northern fringe, both form the main source area of the study formations. This uplift occurred simultaneous to the flexural subsidence (SSE tilting) of the southern part of the basin, where sedimentary aggradation dominated.

Keywords: Guadalquivir basin, Pliocene, Quaternary, foreland basin, forebulge, neotectonics

1. Introduction

The lower Guadalquivir basin constitutes the sector of the Guadalquivir foreland basin located southwest of Sevilla (Fig. 1). Late Pliocene to Quaternary sediments in this sector of the basin mainly accumulated in two areas, namely the Guadalquivir marshlands and the Abalario high. The Guadalquivir marshlands form a wide flat area, of about 1800 km^2, located a few metres above the sea level in the western and lowest part of the Guadalquivir basin. In this area, the most recent part of the sedimentary filling consists of a sequence of flat-lying Plio-Quaternary deposits, up to 400 m thick, that accumulated from alluvial, estuarine and marsh sedimentary environments. The shallowest sediments of this sequence, which are mainly Holocene in age, have been extensively studied by Menanteau (1979), Zazo et al. (1994, 1999a), Rodríguez-Ramírez (1998), Rodríguez-Ramírez et al. (1996a, 1996b, 2001), Lario et al. (2001, 2002), Carretero et al. (2002), Ruiz et al. (2004, 2005), and Pozo et al. (2008, 2010). These authors made a detailed reconstruction of the sedimentary environments, discussed their evolution with regards to climate and sea-level changes, and provided a robust chronological framework based on radiocarbon dating. To the west of the Guadalquivir marshlands, the Abalario constitutes a coastal topographic high of about 450 km^2, made up by aeolian sands that are Late Pleistocene to Holocene in age. These sands crop out along the up to 100 m high and 30 km long Asperillo coastal cliff. The stratigraphic, sedimentologic and petrologic features of this cliff have been the focus of the studies by Caratini and Viguier (1973), Leyva and Pastor (1976), Flor (1990), Borja and Díaz del Olmo (1992), Dabrio et al. (1996), and Zazo et al. (1999b, 2005, 2008). The Abalario sands extend over the southernmost part of the Guadalquivir marshlands, constituting the currently active Doñana spitbar (Rodríguez-Ramírez et al., 1996b).

Bellow these more recent sediments, which constitute the Guadalquivir marshlands and the Abalario high, there is a less known sequence of Pliocene and early

Quaternary sediments drilled during several hydrogeology campaigns (FAO, 1970; IRYDA, 1976; IGME, 1983). Knowledge on these sediments is, however, restricted to their basic lithostratigraphic characteristics (Salvany and Custodio, 1995) for the following reasons: 1) the destructive method used to drill the boreholes, which enabled just a rough description of the sediments recovered; 2) the unequal distribution of boreholes, which are concentrated in the northwestern part of the marshlands (irrigated land) but are almost absent along the eastern margin of the Guadalquivir River (area of brackish groundwater) and the linking zone with the Abalario high (restricted area of the Doñana National Park), thus preventing a detailed correlation between different areas. Such correlation became even more difficult because of the frequent and complex lateral changes in sedimentary facies; and 3) the lack of biostratigraphic markers, which prevent development of an independent chronostratigraphic framework.

During the last decade, the IGME (Geological and Mining Institute of Spain) has drilled several exploratory boreholes in different points of the Guadalquivir marshlands and the Abalario high (Fig. 1) in an effort to gain insights on the lithostratigraphy, sedimentology and chronology of the Plio-Quaternary sediments. Most of these boreholes, which reach down to 300 m, were drilled with continuous core sampling to recover unaltered material suitable for detailed sedimentary studies. In this paper we present the first detailed description of the sediments in these boreholes, define lithostratigraphic units, and bring new chronologic data based on radiocarbon and magnetostratigraphic dating. This information, combined with a complete revision of the older hydrogeological boreholes, is used to propose a new lithostratigraphic and chronologic framework for the whole Plio-Quaternary sedimentary sequence and to establish the paleogeographic evolution of the western part of the Guadalquivir basin in its geodynamic context as the foreland of the Betic Cordillera.

2. Geological setting

The Guadalquivir basin in southern Spain is an ENE-WSW elongated foreland basin developed during the Neogene and Quaternary between the external zones of the Betic Cordillera to the south and Sierra Morena (Iberian Massif) to the north (Sanz de Galdeano and Vera, 1992), which respectively form its active and passive margins (Fig. 1). The basin started to develop during the Middle Miocene in response to flexural subsidence of the Iberian Massif caused by the stacking of allochthonous units of the Betic Cordillera during the convergence between the Iberian and African plates (Sierro et al., 1996; Fernández et al., 1998; Civis et al., 2004; García-Gastellanos et al., 2002). The external zones of the Betic Cordillera are made up of Mesozoic and Cenozoic sediments that include thick calcareous and evaporitic formations, as well as siliciclastic units. Sierra Morena comprises in Paleozoic igneous and metamorphic rocks. These rocks constitute the basement of the Guadalquivir basin, which gradually increases its depth toward the SSE so that it is found 5000 m below the Betic thrust front (Fernández et al., 1998; García-Castellanos et al., 2002).

In the lower Guadalquivir basin, the lowermost unit of the sedimentary filling of the basin is the Niebla Calcarenite Formation (Civis et al., 1987; Baceta and Pendón, 1999). This formation is made up of up to 30 m of gravel, fossil-bearing sand and limestone accumulated in alluvial and coastal environments. It covers an old erosive surface on the Paleozoic basement. The Niebla Calcarenite Formation is overlain by the Gibraleón Clays Formation (Civis et al. 1987), also know in the literature as Blue Marls, which forms a monotonous marly sequence accumulated in a deep marine through formed at the foothill of the Betic Cordillera. This formation increases its thickness from the northern margin of the basin, where it reaches a few tens of metres, to its southern margin, where it reaches more than 1000 m and includes subordinate sand beds (Perconig and Martínez-Díaz, 1977; Martínez del Olmo et al., 2005). This thicker part hosts the so-called allochthonous units (traditionally called “olistostromic units”), which consist of Triassic evaporites and are related to thrusting along the Betic Cordillera deformation front (Berástegui et al., 1998). The Gibraleón Clays Formation is overlain by the Huelva Sands Formation (Civis et al., 1987), made up by up to a few tens of metres of fossil-rich marls, sands and sandstones accumulated in a shallow marine environment. The Huelva Sands Formation is overlain by the Bonares Sands Formation (Mayoral and Pendón, 1986-87), made up by up to a few tens of metres of sands and subordinate levels of gravels accumulated in a coastal environment. The abundant microfaunal content of the upper part of the Niebla (Civis et al., 1987), Gibraleón (Magne and Viguier, 1974; Sierro, 1985), and Huelva (Ruiz-Muñoz et al., 1997) formations has yielded Tortonian, Late Tortonian to Late Messinian, and Late Messinian to Early Pliocene ages for these formations, respectively. No biostratigraphic data are available for the Bonares Formation, tentatively dated as Middle-Late Pliocene-Early Quaternary on the basis of its stratigraphic position above the Huelva Formation (Mayoral and Pendón, 1986–87).

The overlying sediments, of uncertain Plio-Quaternary age, have a more varied geographical distribution and sedimentological significance. In the northern part of the basin, they form a characteristic red coarse alluvial deposit that caps the top of many hills and has a maximum thickness of about 10 m. This deposit was named High Alluvial Level by Pendón and Rodríguez-Vidal (1986–87) and Red Formation by Torres-Perezhidalgo et al. (1977a, 1977b), which are respectively located in the western part and the north-central part of the basin (Fig. 1). They also constitute the old alluvial terraces linked to the evolution of the current drainage network (Salvany, 2004). In the southern part of the basin, three main Plio-Quaternary units were early identified by Salvany and Custodio (1995) from borehole data: an older Alluvial Unit, made up of gravel, sand and clay, about 200 m thick, and two younger coeval units: the Marismas Unit, which is a clayey unit of estuarine origin of up to 60 m thick, and the Aeolian Unit, a sandy unit that reaches a thickness of 150 m. The development of these two younger units leads to the formation of the marshlands area and the Abalario high, respectively.

The structure of the Plio-Quaternary deposits of the lower Guadalquivir basin remains a controversial subject. Some authors identify two sets of normal faults linked to an assumed Pliocene extensional phase, namely a main group of N-S oriented faults that includes the lower Guadalquivir, Guadiamar and Odiel faults, and a subordinate system of E-W oriented faults that mainly developed in the westernmost part of the basin (Armijo et al, 1977, Viguier, 1977). Later studies by Goy et al. (1994, 1996) and Zazo et al. (1999a, 2005), describe similar faults that controlled the more recent sedimentation in coastal areas during the Quaternary. On the other hand, studies by Flores-Hurtado and Rodríguez-Vidal (1994) and Salvany (2004) describe a regional tilting of the basin toward the SSE as the dominant structural feature controlling the sedimentation, and do not identify the fault pattern envisaged by other authors.

3. Data and methods

3.1. Studied boreholes

We have studied the sedimentary sequence recovered from the 22 exploratory boreholes drilled by the IGME in the Guadalquivir marshlands and the Abalario high between 1999 and 2008 (Table 1, Fig. 1). The study is further completed with the VPL borehole (250 m deep) drilled in 2008 by a private company in the Veta La Palma property. These boreholes were mainly drilled by a direct circulation rotary method with continuous core sampling (Cruse, 1979). This method supplies unaltered material, enabling detailed lithologic logging, and is suitable for analytical determinations, such as radiocarbon and magnetostratigraphic dating. The occurrence of intervals made up by loose sand and gravel made this type of drilling unfeasible, so they were drilled using a roller bit with a direct circulation of fluids. In this case, cuttings come up through the annular space between the borehole and the rotating drill pipes, providing a mixture of sediments that might include material dragged from the borehole walls thus a rough identification of the lithology. Boreholes HT, CL and VPL were totally drilled by a roller bit of large diameter with a reverse circulation of fluids, where the cuttings come up inside the drill pipes lessening mixtures. This method generates cuttings large enough for a reasonably good description of the lithology but not for analytic determinations.

The 23 studied boreholes sum a total length of 5253.85 m. Except for HT, CL and VPL, 70.4% of the total borehole length corresponds to pristine sediments drilled with continuous core sampling, and the rest corresponds to cuttings drilled using other methods. This ratio varies between 100% in eight boreholes and 29.3% in borehole F1.

Additionally, the lithologic-logs of a total of 580 old hydrogeologic boreholes were revised. These boreholes were all drilled using a roller bit, some times with direct circulation and others with reverse circulation of fluids. They provide lithologic-logs of variable quality. In general, boreholes drilled with reverse circulation of fluids supplied lithological information of reasonable good quality for the purpose of our study.

The location of all lithostratigraphic and analytical data within the studied boreholes is marked by their position with respect to the surface and is referred to as metres below the surface (mbs).

3.2. Radiocarbon data

To date the uppermost sediments of the marshlands, a total of 17 samples of organic matter were analyzed using the ^{14}C method (Table 2). Samples were taken from different boreholes, where the organic remains appear as black layers of peat or scattered fragments of wood or charred material. In all cases, samples correspond to organic-rich material in enough amounts to ensure reliable data. This is especially the case in peat layers, where the organic matter is an abundant material easy to separate in the laboratory from its siliciclastic host sediment. The fragments of wood and charred material have common sizes up to few centimetres. Once separated from their host sediment, these isolated fragments become very pure organic remains of good quality for radiocarbon analysis.

Most of these samples were analysed following the AMS method in the Beta Analytic Laboratory in Florida (USA) and the Poznan Radiocarbon Laboratory in Poland. To support the paleomagnetic data described below, and in view of the important development of peat layers in its uppermost part, the LE borehole was sampled in more detail.

3.3. Paleomagnetic data

In order to provide a chronological constraint for the studied formations, we have performed a magnetostratigraphic study of the LE borehole. This borehole was chosen because it covers the most complete sequence of fine-grained Pliocene and Quaternary sediments suitable for paleomagnetic analyses, and includes the thickest sequence of recent marshlands deposits suitable for radiocarbon dating. A total of 98 paleomagnetic samples were drilled perpendicular to the borehole sections using a standard petrol-powered drill. Paleomagnetic sampling focused on fine-grained lithologies such as clays and fine-grained sands, and avoided coarser-grained lithologies, less useful for paleomagnetic analyses. The sampled section includes the whole uppermost 270 m of the LE borehole, with the exception of a 23 m interval of unconsolidated sands and gravels between 76 and 99 mbs. This has resulted in a homogeneous sampling with a mean resolution of about 2.1 m. Sediments below 270 mbs could not be drilled due to the unconsolidated nature of the mostly coarse bioclastic sands.

Paleomagnetic analyses were carried out using a 2G superconducting rock magnetometer at the Paleomagnetic Laboratory (SCT-UB/CSIC) of the Institute of Earth Sciences Jaume Almera in Barcelona (Spain). The noise level of the magnetometer is less than 7 x 10^{-6} A/m, much lower than the magnetization of the measured samples. Thermal treatment, which was conducted using a MMTD–80 furnace, involved between 8 and 12 steps at intervals of 100°, 50°, 30° and 20°C to a maximum temperature of 680°C. Demagnetization of a set of pilot samples representative of all the lithologies studied allowed optimizing the demagnetization steps and thus the accurate calculation of the magnetization directions that minimize the heating and formation of new magnetic phases in the oven. Stable Characteristic

Remanent Magnetization (ChRM) directions were identified through visual inspection of orthogonal demagnetization plots (Zijderveld, 1967), and were calculated by means of Principal Component Analysis (Kirschvink, 1980).

4. Results

4.1. Lithostratigraphy

The lithologic logs of the studied boreholes has enabled identification of a lower marine sequence, made up of fossil-bearing marly and sandy sediments of characteristic grey colour, and an upper continental to restricted marine sequence consisting in gravels, sands and clays that display a variety of colours and have a low marine fossil content. The first sequence includes the Neogene sediments of the Gibraleón and Huelva formations. The lithostratigraphy, sedimentology and chronology of these formations are described in detail in studies cited above, so they are not further discussed. The second sequence includes the overlying, newly defined Almonte, Lebrija, Abalario and Marismas formations, whose main lithological characteristics are described next.

4.1.1. Almonte Sands and Gravels Formation

This formation constitutes a coarse clastic unit made up by gravels, sands and occasional clayey and marly intervals, and is orange, yellow and, less frequently, grey (Figs. 2, 3 and 4). In the marshlands area, this unit has a thickness that increases southward from 10 to 110 m. In this same southward direction, the grain size of gravels tends to decrease, and the sediments grade from sandy gravels to dominant sands with minor gravel beds. Both gravels and sands are loose, lack a clayey matrix, and have grain shapes that range from well rounded to subangular. Gravel grains reach more than 10 cm in size, with more common grain sizes, between 1 and 5 cm. They are of metamorphic and igneous composition, dominantly quarzose in nature, although fragments of schists, hornfels and porphyrs are also present. Sand grains are mainly of quartz composition, with variable amounts of plagioclase, alkali feldspars, and rock fragments. This composition indicates that the source area was located north of the basin, in the Sierra Morena, because no metamorphic and igneous rocks are found in the Betic margin. The lower boundary of this formation is represented by a gradual transit from the underlying Huelva Formation in the south-eastern part of the marshlands (boreholes MA, PN, SL and LE). Toward the northern and western part of the marshlands, this boundary is an erosive surface developed on the Huelva Formation.

In the Abalario area, the Almonte Formation is a thin homogeneous layer that reaches 26 m thick in the LJ borehole (Fig. 2). It constitutes a fining-upward sequence with an erosive basal surface that cuts the underlying Huelva Formation. The fact that the alluvial sediments were not drilled in most of the boreholes, in the transition between the Abalario and the marshlands, suggests the existence of a gentle paleorelief originated during the down cutting phase previous to their sedimentation (Fig. 5, cross-section 5).

The Almonte Formation records the development of a wide, alluvial system that drained the Sierra Morena and extended beyond the current coastline. It represents the onset of continental deposition in the Guadalquivir basin, which followed the long episode of marine sedimentation persistent in the basin since the Tortonian (Late Miocene).

4.1.2. Lebrija Clays and Gravels Formation

This formation is made up of clays with subordinate sand and gravel beds that have a variable vertical distribution at different locations (Figs. 2, 3 and 4). The formation can be divided into two units. The lowermost one is made up by brown and greenish clays that have either a visually massive or a laminated structure. Massive clays contain common root marks and white carbonate nodules. Laminated clays are made up of an alternation of thin fine-grained sandy and clayey layers. Occasional marine shells of gastropods and bivalves are also found. Sands have a clayey matrix, range from fine to coarse grain size, and include subordinate gravel layers and many scattered mud-clasts. Gravels contain well-rounded clasts of up to 10 cm in size, and include variable fractions of a clayey and sandy matrix. Gravels form layers of several metres in thickness with a fining-upward structure, and have a rare lateral continuity between adjacent boreholes (paleochannels). Clasts and sand grains are dominantly quarzose and metamorphic in composition, similar to that described above for the Almonte Formation. This lower unit extends throughout the southern part of the studied area, and increases its thickness towards the southeast, reaching a maximum thickness of 120 m at the LE borehole (Fig. 3). In this borehole, the unit is directly overlying the Huelva Formation. However, towards the north and west, it gradually expands over the sediments of the Almonte Formation (Fig. 5).

Sediments of this lower unit can be interpreted as distal alluvial sediments accumulated on a muddy alluvial plain crossed by gravel-bearing fluvial channels sourced in the Sierra Morena. The root traces and carbonate nodules suggest wide spread development of vegetation on the muddy plain. Although the main sediments indicate an alluvial environment, occasional marine bivalve shells might indicate some sporadic marine influence in the southern part of the basin. This lower unit of the Lebrija Formation can be considered as the distal sediments of the Almonte alluvial system (Fig. 5).

The upper unit of the formation is a fining-upwards sequence of coarse gravels at the base, gravels and coarse-grained sands in the middle part, and coarse- to fine-grained sands towards the top. It forms a continuous bed throughout most of the northern half of the marshlands. In the northernmost boreholes (SE, MJ, F1 and F4), this unit cuts the Almonte Formation, while in the other boreholes it grades over the lower unit of the Lebrija Formation. In the northern part of the marshlands the upper unit has a rather constant thickness of 10 to 15 m that reaches 22 m at the LE borehole (Fig. 3). However, toward the south it becomes thinner (PN, VPL, MA boreholes) and it is even locally absent (VP) (Fig. 5). Again, the dominant quartzose and metamorphic composition of pebbles and sands indicate a northerly provenance in the Sierra Morena. Due to its loose and coarse-grained nature, sediments of this upper unit were drilled using the roller bit. Therefore, only a basic lithologic description based on cuttings is available.

Sediments of this upper unit can be interpreted as proximal alluvial sediments that throughout the northern part of the study area rapidly prograded over the Almonte Formation and the lower unit of the Lebrija Formation (Fig. 5).

4.1.3. Abalario Sands Formation

This formation (formerly the Aeolian Unit of Salvany and Custodio, 1995) is a thick package of homogenous medium- to fine-grained sands that lack of a clayey matrix and are white, yellow and orange (Figs. 2 and 4). Sands are mainly quartz, but include feldspars and heavy minerals that form thin, black laminae (Caratini and Viguier, 1973; Leyva and Pastor, 1976). The lack of fossils is another significant feature of their composition. Sands are occasionally cemented by iron oxides in nodules and hard crusts up to several centimetres thick, which have a characteristic reddish colour. The formation shows a maximum thickness of 150 m in the southeastern part of the Abalario high, and thins progressively to the north and west.

The sediments of the Abalario Formation originated from an aeolian system that prograded NW to SE following the shoreline. According to Caratini and Viguier (1973), the sands were supplied by reworking of the Late Pliocene sediments under denudation in the northern margin of the basin. The aeolian origin of these sediments was mainly documented in the Asperillo coastal cliff. Along this cliff, typical aeolian cross-beds are exposed together with thin iron-oxide crusts, paleosoils and carbon-rich layers (Flor, 1990; Borja and Díaz del Olmo, 1992; Dabrio et al., 1996; Zazo et al., 2005). The cliff cuts ancient dunes originally developed several hundred of metres inland. Related beaches of this aeolian system were completely eroded by the sea waves and reworked into the spitbar of Doñana (Rodríguez-Ramírez, 1998). Bellow the cliff, the lower sands of the Abalario Formation display the same lithofacies. This suggest that the aeolian system developed continuously from the beginning of the formation, first covering the alluvial sediments of the Almonte Formation and then onlapping over the lateral equivalents of the Lebrija and Marismas formations (Fig. 5, cross-section 5). Such lateral gradation is supported by the sediments drilled between the Abalario and the marshlands at boreholes TC, SO, and CL, where aeolian sands intercalate frequent grey or greenish clay beds, often with carbonate nodules, root molds and vegetal remains that are wedges of the adjacent Lebrija and Marismas clayey formations. Today, aeolian dunes are only active at the Doñana spitbar. Elsewhere the aeolian areas are inactive and are being eroded (Flor, 1990; Dabrio et al., 1996).

4.1.4. Marismas Clays Formation

This formation is made up of a characteristic dark grey or brown homogenous clay that includes minor clayey sandy layers of fine to medium grain size (Figs. 2, 3 and 4). The clays and sands commonly are laminated and contain organic matter. Shells of bivalves, gastropods, echinoderms, and other marine fauna are commonly found scattered or concentrated in coquina layers several centimetres thick. Closed bivalve shells are often found along with unbroken shells of other marine fauna, indicating a very low energy environment. Organic mater appears either diffuse within the sediments or concentrated in peat layers of few centimetres thick. Black vegetal roots and wood fragments are also frequently scattered within these sediments. Occasional paleochannels of gravel and coarse-grained sand interbedded within the clays are present in the LE and HT boreholes.

The thickness of the Marismas formation gradually increases from north to south, from less than 20 m in boreholes MJ and SE to 79 m in LE borehole (Figs. 2 and 3). The sand content increases significantly in the same direction, even to the point of exceeding the clay fraction. The lower boundary of this formation in the central part of the Guadalquivir marshlands is a gradual contact over the underlying upper unit of the Lebrija Formation. As a local feature, the Marismas clays reach a large development in the south-eastern edge of the marshlands (borehole CM, Figs. 4 and 5). In this case, it is considered that a substantial part of this sequence could represent a lateral gradation of the more distal sediments of the Lebrija Formation. The upper boundary of the Marismas Formation corresponds to the surface of the marshlands, where sedimentation continues.

The Marismas Formation represents a marine transgression that expanded over the previously deposited alluvial sediments of the Lebrija Formation. It is a shallow marine deposit that filled an estuary developed in the present-day marshland area. Clay intervals can be interpreted as muddy lagoon sediments, while sands would represent sandbars, beaches or sandlflats developed around the lagoon. In the north-western part of the marshlands (boreholes MJ, F1, F4 and HT), the Marismas Formation forms a homogenous clayey sequence that suggests the development of a relatively stable lagoon. In the eastern part of the marshlands (boreholes VPL, VP, LE, PE and SE), the Marismas Formation constitutes a transgressive sequence made up with a lower sand layer, without fossil remains; an intermediate interval, where marine shell-bearing clay and sand layers alternate, and an upper clayey layer that contains common marine shell. The lower sands of this sequence can be interpreted as distal alluvial sediments coming from the northern part of the basin (the mouth of the early Guadalquivir River). Upward, marine sediments gradually developed, first as sandflat and beach sediments and later as lagoon sediments. In the southern part of the marshlands, the Marismas Formation constitutes a sandy sequence with minor clayey layers (boreholes PN and MA). Toward the south-east, sand layers become less frequent (borehole SL), even non-existent (borehole CM). This area can be interpreted as a coastal sandy barrier that prograded toward the SE. The barrier sands were supplied by reworking the aeolian sands of the Abalario area. This source agrees with the similar quarzose composition of both the Abalario and Marismas sands. Development of this barrier leads to the formation of the spitbar of Doñana, which closed the estuary and formed the present-day marshlands.

4.2. Radiocarbon data

All samples located at less than 40 mbs in every borehole sampled have radiocarbon ages younger than 9600 ± 50 years BP (Table 2). Two additional samples located between 50 and 60 mbs in the VP and TC boreholes have ages ranging from 29880 ± 280 to 45460 ± 1900 years BP. At levels deeper than 60 mbs, all available ages are beyond the range of radiocarbon dating. The exception to this pattern is the PN borehole, where ages beyond the range of the radiocarbon method are found at a depth of 35.5 mbs (Table 2).

4.3. Magnetostratigraphy

In most samples, two stable components are present. A low-temperature component is unblocked below 225–300ºC. This component shows either steep directions of around 50–60º (Fig. 6 A, C), interpreted as present-day field overprints, or shallow directions broadly perpendicular to the borehole sections (Fig. 6 D, I), interpreted as acquired during drilling. Above 225–300ºC, a ChRM can be identified in about 95% of the samples. The behaviour of the ChRM depends on lithology. The ChRM in grey clays and fine-grained sands from the Marismas and Huelva formations shows maximum unblocking temperatures of up to 500º C (Fig. 6 A, B, G, I), which points to magnetite as the main magnetic carrier. In clays and fine-grained sands from the Lebrija Formation, the maximum unblocking temperature of the ChRM ranges between 420º and 650º C, indicating that hematite is also a common magnetic carrier.

Based on demagnetization pattern, ChRM directions were divided into three groups. Type 1 ChRMs are those that describe well-defined linear trends that enable the accurate calculation of their directions and optimum polarity determinations (Fig. 6

A, C, E, G). Type 2 ChRMs are those that either display less-developed linear trends or incomplete demagnetizations due to the growing of new magnetic minerals in the oven. Nevertheless, they provide reliable polarity determinations by fitting selected or clustered directions to the origin of demagnetization plots (Fig. 6 D, F, H). Type 3 ChRMs are those that display clustered directions that might provide ambiguous polarity determinations (Fig. 6 I). About 43, 42 and 15% of ChRM directions belong to Quality Types 1, 2, and 3, respectively.

ChRM shows both positive and negative inclinations regardless of lithology. The mean of the negative ChRM directions is –38.9º ± 21.2º, a few degrees shallower than the mean of the ChRM normal directions (+45.9º ± 20.2º) and likely results from a stronger overlap of negative ChRM directions with the present-day field overprint. The means of both positive and negative ChRM directions are slightly shallower than the expected inclination for the studied site (around ±50º), which is consistent with a detrital origin for ChRM. In any case, both positive and negative ChRM mean directions are statistically consistent with the expected inclination, which suggests, together with the lack of a lihological control on ChRM directions, that ChRM provides a reliable record of the polarity reversals of the geomagnetic field.

Because the azimuth of the borehole is unknown, plus the need for quality, the identification of polarity zones was solely based on the inclination of Type 1 and 2 ChRM directions (Fig. 7). Nevertheless, most Type 3 ChRM directions appear to be consistent with those of Types 1 and 2. The established succession of polarity reversals includes 5 normal magnetozones, here labelled N1 to N5 from top to bottom, and 5 reverse magnetozones, here labeled R1 to R5 (Fig. 8). Each magnetozones was determined by at least two consecutive samples, averaging a total of 7.8 samples per magnetozone. Short intervals of only one sample, which might correspond to chryptochrons, were not considered. The most conspicuous patterns of the Lebrija borehole polarity sequence are a long normal polarity interval in the upper part of the section (N1), two reverse magnetozones (R1, R2) separated by a short normal interval

(N2) in the centre of the section, and a cluster of three short normal magnetozones (N3 to N5) separated by two short reverse intervals (R3, R4) in its lower part (Fig. 7).

5. Discussion

5.1. Chronology of the Plio-Quaternary sedimentary sequence

Radiocarbon data enable identification of Holocene ages (i. e., < 11.5 Ka BP) to a depth of 17.5, 28.9 and 37.6 mbs in PN, PE and LE boreholes, respectively (Table 2). On the other hand, Late Pleistocene ages of 29880 ± 280 and 45460 ± 1900 years BP are found at depths between 50 and 60 mbs in TC and VP boreholes. Bellow 60 mbs, all ages are beyond the range of radiocarbon dating. In an earlier study, Zazo et al. (1999a) provided three radiocarbon ages from shells from the Mari López borehole, drilled in the Guadalquivir marshlands 6 km southwest of HT borehole. Two samples taken at 7.3 and 10.8 mbs gave Holocene ages younger than 6000 years BP, whereas a third sample collected at 27.5 mbs gave a Late Pleistocene age of 47400 ± 3100 years BP. The study by Pozo et al. (2010) provided five radiocarbon ages from shells from the PLN (Palacio de Las Nuevas) borehole, close to the PN borehole of our study. Four samples, taken above 25 mbs gave Holocene ages younger than 7000 years BP. The fifth sample collected at 55.3 mbs gave a Late Pleistocene age of 43370 ± 960 years BP. Additional radiocarbon ages from shells of less than 5000 years BP taken from the shallowest sediments of the southwest area of the marshlands were provided by Ruiz et al. (2004 and 2005).

Overall, these results place the Pleistocene-Holocene boundary within the Marismas Formation deeping eastward from around 11 mbs in the Mari López borehole (Zazo et al., 1999a) to 40 mbs in the Lebrija borehole (LE). They also indicate that ages beyond the range of radiocarbon dating, and hence older than approximately 50000 years BP, are present at variable depths between about 30 mbs in the Mari López and PN boreholes and 60 m in LE, VP, and TC boreholes.

The correlation of the polarity sequence established for LE borehole with the revised astronomically-tuned Neogene timescale (ATNTS2004 of Lourens et al., 2004 and Gradstein et al., 2004) is straightforward based on the characteristic pattern of magnetozones, on available radiocarbon ages for the Marismas Formation, and on biostratigraphic constraints for the Huelva Formation. Radiocarbon ages of < 11.5 Kyr BP in the uppermost part of the long N1 interval constraint it to correlate with those of Brunhes (C1n) chron (Fig. 7). This implies that the underlying, predominantly reverse interval (R1 to R2) must correlate with the Matuyama period (chrons C1r to C2r), so that the characteristic cluster conformed by intervals N3 to N5 corresponds to the predominantly normal Gauss (C2.An) chron and the underlying R5 interval correlates to the top of the Gilbert (C2Ar) period. This correlation is supported by biostratigraphic data indicating an Early Pliocene age for the Huelva Formation (Sierro et al., 1996). The short N2 interval can be correlated either to the Jaramillo (C1r.1n) or to the Olduvai (C2n) events of the Matuyama period (Fig. 7). Since no evidence of a sedimentary hiatus was observed in the upper part of the upper unit of the Lebrija Formation, the best match is provided by the correlation of N2 to the Olduvai chron (Fig. 7). This interpretation implies that most of chron C1r (including the Jaramillo event) is either missing below, or represented within the 22 metres-thick package of unconsolidated gravels and coarse-grained sands that made up the upper unit of the Lebrija Formation.

The radiocarbon and magnetostratigraphic results enable determinating the ages and mean accumulation rates for the formations, and estimating on the age and duration of the sedimentary gap around the upper unit of the Lebrija Formation (Fig. 7). Mean accumulation rates of about 350 cm/Kyr for the Holocene part of the Marismas Formation in LE borehole can be estimated keeping in mind the position of the Pleistocene-Holocene boundary at about 40 mbs. Toward the west, this accumulation rate decreases down to about 95 cm/Kyr as the depth of the Pleistocene-Holocene boundary reaches shallower positions of around 11 mbs (i. e., Mari López borehole).

For the lower part of the Marismas Formation, a mean accumulation rate of about 50 cm/Kyr can be established for all boreholes on the basis of location, at variable depths between 30 (in the Mari López and PN boreholes) and 60 mbs (in LE, VP, and TC boreholes), of ages beyond the range of radiocarbon dating. The linear extrapolation of this accumulation rate downwards from the position of the Pleistocene-Holocene boundary results in an estimated Late Pleistocene age between 85 and 110 Ka for the base of the Marismas Formation.

Concerning the Lebrija Formation, the age of its base can be constrained at ~3.7 Ma. A mean accumulation rate of around 6 cm/Kyr can be established for this formation between the lower boundary of chron C2An and the top of the Olduvai chron (C2n) in LE borehole. However, these are just mean accumulation rates that might have larger and smaller values. This situation is clearly illustrated in the lower part of the formation, where the presence of several polarity reversals within chron C2An demonstrates that accumulation rates oscillate from <1 to >10 cm/Kyr. Something similar is found between 99 and 110 mbs, where the presence of the Olduvai chron enables estimating accumulation rates as low as 1.2 cm/Kyr. Such highly variable accumulation rates over short time intervals are attributed to the nature of the coarse-grained intervals within the Lebrija Formation, which are characterized by channel-like geometries involving periods of either erosion or no deposition. The extrapolation of the linear accumulation rates upwards from the top of the Olduvai event in LE borehole yields an estimated age of about 1.6 Ma for the top of the lower unit of the formation (Fig. 7). In view of the transitional contact between the top of the upper unit of the Lebrija Formation and the base of the Marismas Formation, which is dated at about 100 Ka, a period of up to ca. 1.6 Myr must be represented either within or at the base of its upper unit. It is unknown whether this time interval was accommodated by a period of deposition followed by erosion or by a period with very low but continuous agraddation. Given the sharp lower boundary of the upper unit of the Lebrija Formation, and keeping in mind that it represents a widespread expansion of alluvial sedimentation over different underlying formations, the first option seems more likely. In that case, an age of ca. 300 Ka can be estimated for the base of this upper unit, considering mean accumulation rates of 10 cm/Kyr that characterize alluvial sedimentation for the rest of the Lebrija Formation. In this case, the temporal gap between the two units of the Lebrija Formation must represent around 1.3 Myr (Fig. 7). With regards to the Almonte Formation, and keeping in mind that this is a lateral equivalent of the Lebrija Formation, variable mean accumulation rates between about 1 and 6 cm/Kyr can be established for this formation.

Concerning the Huelva Formation, no magnetostratigraphic data are available in the LE borehole. Thus, the age of neither its different stratigraphic intervals, nor its base, can be magnetostratigraphically constrained. Nevertheless, the base of the Huelva Formation broadly coincides with the Miocene/Pliocene boundary (Sierro et al., 1996; González-Delgado et al., 2004) dated at 5332 Ma (Lourens et al., 2004; Gradstein et al., 2004). The top of the Huelva Formation lies in the uppermost part of chron C2Ar, and therefore is ~3.7 Ma near the end of the Early Pliocene (Fig. 8). Taking into consideration that the base of the Huelva Formation was not reached in LE borehole at –336 m, a minimum mean accumulation rate of 7 cm/Kyr can be estimated for this formation at LE borehole.

5.2. Correlation with the surrounding northern areas

Based on the results shown above, we provide new insight on the correlation of the Late Pliocene to Holocene sediments between the Guadalquivir marshlands and those deposited in the northern areas of the lower Guadalquivir basin. To the south and east, the lack of subsoil data prevents the establishment of a reliable correlation.

5.2.1. Correlation with the Aljarafe high and the Almonte plain

The Aljarafe is a topographic high area located north of the marshlands, between the Guadiamar and Guadalquivir rivers (Figs. 1 and 8 cross-section A). It constitutes a monocline gently dipping to the south, made up of an up to 30 m-thick sequence of yellowish sands and sandstones. Toward the south, the Aljarafe sands grade laterally to the Huelva Formation, which is buried within the marshlands, beneath the Almonte, Lebrija and Marismas formations. In the southern part of the high, the Aljarafe sands are overlain by a 25 m-thick sequence of red coarse-grained clastic sediments of alluvial origin (the Red Formation of Torres et al., 1977b). These sediments are well exposed in several old quarries along the southern edge of the Aljarafe high. In these quarries well rounded alluvial gravels with coarse pebbles of up to 25 cm in size are shown, in layers that have common paleochannel and cross-bedding structures. Clasts display the same metamorphic and igneous composition as in the Almonte Formation. The sedimentological features of these sediments, coupled with borehole data, indicate that the Red Formation is a lateral equivalent of the Almonte Formation, bellow the Marismas and the upper unit of the Lebrija Formation.

The gentle southward-dipping monocline of the Aljarafe extends further west into the Almonte plain (Figs. 1 and 8 cross-section B). In that area, a 20 m-thick sequence of variegated sands and gravels (the Bonares Formation of Mayoral and Pendón, 1986–87) crops out overlying the Huelva Formation. On the basis of the stratigraphic position of the Bonares Formation, equivalent to Aljarafe sands, this formation is interpreted to constitute a lateral equivalent of the uppermost part of the Huelva Formation. Based on our results, an Early Pliocene age can be inferred for the Aljarafe and the Bonares formations. In the Almonte plain, the lateral equivalent of the Almonte Formation is the High Alluvial Level of Pendón and Rodríguez-Vidal (1986-87). It is mainly represented in the outcrops of the westernmost part of the basin (Fig. 1), where it cuts the Huelva and Bonares formations. The boundary is indeed an erosive surface

The Red Formation and the High Alluvial Level constitute the proximal sediments of the alluvial system that originates the Almonte Formation. Rodríguez-Vidal (1989) interprets such proximal sediments as the ones originated by braided rivers coming from the Sierra Morena, which is consistent with the inferred interpretation for the Almonte Formation.

5.2.2. Correlation with the alluvial terraces of the Guadiamar River

The Guadiamar River is a N-S flowing river that drains the Sierra Morena and the northern part of the lower Guadalquivir basin, where respectively it cuts Paleozoic rocks and Neogene sediments of the Gibraleón and Aljarafe formations before flowing into the Guadalquivir marshlands (Fig. 1). Apart from the present-day alluvial plain (labelled T0), this river developed a system of three terraces labelled T1 to T3 (Salvany, 2004) (Fig. 9). According to radiocarbon dating, T1 and the uppermost part of T2 are Holocene in age. In the lower part of T2, the age is beyond the range of radiocarbon dating (Salvany et al., 2004). Radiocarbon data suggest that T2 correlates with the prominent package of gravels and sands intercalated within the middle part of the Marismas Formation at LE borehole, between 48 and 56 mbs, which also ranges between Late Pleistocene and Holocene in age (Fig. 9). In the upper part of the Guadiamar valley T3 is located about 25 m above T1 and T2. This height gradually decreases toward the valley mouth where T3 descends below the younger terraces. In the marshlands area, borehole and chronologic data suggest that T3 is a lateral equivalent of the upper unit of the Lebrija Formation, which is consistent with an inferred Middle Pleistocene age for both units (Fig. 9).

5.3. Tectono-sedimentary evolution

As a whole, the continental Plio-Quaternary sediments of the lower Guadalquivir basin form a wedge-shaped deposit that thickens towards the Betic thrust front of the basin (Fig. 8). The deposit has a basal unconformity overlain by coarse gravels that pass upwards to gravel-bearing clays and then to clays and sands in the upper part. This deposit forms a fining and thinning-upward sequence that can be considered a second-order sequence in the context of the whole infill of the basin. In turn, this sequence consists of three sequences of minor (third) order, each one showing a stratigraphic trend similar to main one (Fig. 10).

Sequence 1 is the lowest and thickest one. It is composed of proximal-alluvial sediments of the Almonte Formation and of distal-alluvial sediments of the lower unit of the Lebrija Formation. Sequence 2 has an intermediate thickness, comprising the proximal-alluvial sediments of the upper unit of the Lebrija Formation and the distal-alluvial sediments of the lower part of the Marismas Formation. Sequence 3, the uppermost and thinnest one, is composed of distal-alluvial, estuarine and marsh sediments of the upper part of the Marismas Formation. The chronostratigraphic data allow dating these sequences respectively as late Pliocene to early Plesitocene (3.7–1.6 Ma), early to late Pleistocene (1.6–0.015 Ma), and latest Pleistocene to present-day (15–0 Ka).

Sequence 1 represents the onset of continental sedimentation in the lower Guadalquivir basin (Fig. 10–1). Its basal erosive surface indicates that an important downcutting period preceded the accumulation of continental sediments. At that time, braided rivers sourced in the Sierra Morena transported coarse clastics throughout the basin, including well beyond the present coastline of the Gulf of Cádiz. Subsequent subsidence of the basin concurred with a retrogradation of the alluvial system, so that the braided rivers that initially spread throughout most of the basin gradually retreated towards the source area.

This sedimentary evolution can be explained in light of the tectonic scenario envisaged for the Guadalquivir basin by García-Castellanos et al. (2002) on the basis of geophysical data and modelling. According to these authors, a substantial part of the present relief of Sierra Morena is related to its uplift as a forebulge of the Betic Cordillera. During the syn-orogenic period (late Serravallian to Tortonian) the Betic thrust wedge loading caused a flexural forebulge in the craton margin of the basin that was onlaped and buried by contemporary marine sediments. Once thrusting ended (post-orogenic period), the viscous relaxation of the lithosphere developed an emergent forebulge migrating southward, narrowing the basin and uplifting its distal sediments. This post-orogenic period started at around 6.5 Ma (early Messinian) and extended throughout the latest Miocene, Pliocene and Quaternary (Berástegi et al. 1998). In the LE borehole, is around 3.7 Ma (Early-Late Pliocene boundary) the first clear evidence of this forebulge uplift. Continued northward retrogradation of the alluvial system between 3.7 and 1.6 Ma likely reflected the progressive denudation of forebulge of the Sierra Morena during a subsequent quiescent phase.

The development of flexural forebulges is a common feature of many foreland basin systems (DeCelles and Giles, 1996; Catuneanu, 2004). In general, it is stated that forebulge uplift occur coeval to foredeep subsidence, both related to thrust loading of an orogenic belt (Beaumont et al., 1988). During an overthrust phase the immediate response of the lithosphere to loading is elastic and results in a downwarped flexural basin adjacent to the orogen and the elevation of a peripheral forebulge along the cratonward edge of the basin. If the thrust load remains unchanged for a long period, viscous relaxation of the plate-bending stress results in deepening of the basin, as well as uplift of the forebulge and its contraction toward the load (Quinlan and Beaumont, 1984; Tankard, 1986; Sinclair et al., 1991).

Sequence 2 is preceded by a new period of downcutting between 1.6–0.3 Ma, which affected the whole basin and likely resulted in the by-pass of sediments towards the present-day offshore of the Gulf of Cádiz. This erosive event is linked to a new period of forebulge rebound of the Sierra Morena, developed together with a significant migration of the forebulge into the basin. This reflects the viscous relaxation phase envisaged in the model of Garcia-Castellanos et al. (2002) (Fig. 10–2). Hereby, the hinge line that delimits forebulge and foredeep shifted toward the SSE at least 40 km. This line became a tilt axis from which the marshlands area sank as the northern part of the basin uplifted.

The uplift of the northern part of the basin triggered the reworking of continental sediments accumulated in the previous sequence (i. e., the High Alluvial Level and the

Red Formation), which then started to develop as a denudation plain gently dipping towards the SSE. The Neogene deposits of the northern part of the basin were exhumed and also reworked into the basin. After de erosion, a relatively sudden spread of alluvial sediments developed throughout the northern part of the marshlands area. Alluvial sediments of the upper unit of the Lebrija Formation were supplied by the early Guadiamar River, which, at the same time, developed terrace T3, as well as by its contemporary Guadalquivir River. The distal part of the alluvial system gave way to the lowermost sediments of the Marismas Formation, which gradually expanded northward over the proximal alluvial sediments. This system was bounded to the east by the Abalario sands, which prograded south-eastward starting early in the first sequence.

The third sequence is characterized by the development of terrace T2 in the Guadiamar valley. The development of this terrace was preceded by a third period of dawn-cutting, which left remains of terrace T3 on the surrounding hills. Beyond the Guadiamar valley, the erosion was restricted to the easternmost part of the marshlands, where some alluvial channels were excavated through the uppermost sediments of the preceding sequence (Fig. 10-3). This sequence would represent a last smaller pulse of the Sierra Morena.

Since 6 Ka, this uppermost sequence witnessed a marked transgression so that marine restricted facies (i. e., the upper part of the Marismas Formation) accumulated in an estuary that was bounded by tidal flats and minor distal alluvial plains near the mouth of the Guadiamar River, which then developed terrace T1, and the Gualdalquivir River (Fig. 10–4). In historical times, the SSE progradation of the Doñana spitbar in the south-easternmost tip of the Abalario led to the closure of the estuary to the open sea, giving way to the present-day marshland environment (Rodríguez-Ramírez, 1998). The last 300 years have witnessed a last incision of the fluvial network, resulting in the formation of terrace T0 along the Guadiamar valley (Salvany, 2004) and in the development of small deltas built by the main streams flowing into the marshlands (Bayán and Dolz, 1995).

The influence of forebulge dynamics in basin infilling are documented in many studies (Heller et al., 1988; Fleming and Jordan, 1990; Sinclair et al., 1991; Plint et al. 1993; Crampton and Allen, 1995; Catuneanu and Sweet, 1999). In general, as occurred in the study case and agreeing with our interpretation, these studies demonstrate that each phase of forebulge uplift leads to an unconformity on its flanks and the shift of the sedimentary facies. Subsequent denudation of the emerged forebulge normally supplies the basin with clastic sediment with the main sedimentary infill coming from denudation of the thrust area (Heller et al., 1988; Fleming and Jordan, 1990; Plint et al., 1993). In the study case, the lithology of the pebbles and sand shows that they dominantly were supplied from the craton margin of the basin. The apparent lack of sediments coming from the thrust area is difficult to understand, and is not resolved in our study. Probably, the present-day marshlands represent only a small part of the Plio-Quaternary foredeep, whose proximal part remains partially hidden below more recent thrust-sheets where subsoil data are unavailable.

The explained tectono-sedimentary evolution of the lower Guadalquivir basin suggests a late Pliocene to Quaternary decreasing uplift of the Sierra Morena forebulge, related to a coeval decrease of the contractional deformation of the Betic orogen. This contractional deformation would be generated by a NNW-SSE compression that persisted along this period, which is consistent with the regional tectonic studies that deal with the Betic Cordillera and related Guadalquivir foreland basin (Galindo-Zaldívar et al., 1993; Morales et al., 1999).

6. Conclusions

This study dates the onset of continental sedimentation in the lower Guadalquivir basin at the Early Pliocene-Late Pliocene boundary as 3.7 Ma in the LE borehole. Since then, the basin has mainly filled by alluvial sediments of the Almonte and Lebrija formations and the lower part of the Marismas Formation, as well as by aeolian and shallow marine sediments of respectively the Abalario Formation and the upper part of the Marismas Formation. These formations form three fining-upward depositional sequences that attest to the uplift of the craton side of the basin (i. e., the Sierra Morena) as a forebulge of the Betic Cordillera and to the simultaneous greatest subsidence of the basin along to the Betic deformation front. From radiocarbon and magnetostraigraphic data, these sequences are dated Late Pliocene to Early Pleistocene (3.7–1.6 Ma), Early to Late Pleistocene (1.6–0.015 Ma), and latest Pleistocene to present-day (15–0 Ka).

Each sequence is characterized by: first, an initial period of down-cutting that produced a regional unconformity; second, a rapid alluvial progradation supplied by the craton margin of the basin along the thrust front; and third, a slow alluvial retrogradation cratonward. In the third sequence, retrogradation occurred together with a shallow marine transgression that flooded the southern part of the basin. The rapid alluvial progradation of the first and second sequences attest to two main periods of increased forebulge uplift at 3.7 Ma and 1.6-0.3 Ma. A period of minor uplift at the Pleistocene-Holocene boundary is represented by the basal erosion of the third sequence. The subsequent episodes of slower alluvial retrogradation reflect decreased forebulge uplift and its denudation.

In most foreland basins, the facies architecture and sediment supply are largely controlled by the adjacent orogenic belt some distance from the craton. In contrast, the late evolution of the lower Guadalquivir basin at least since Late Pliocene was mainly controlled by tectonic uplift and sediment supply from the craton side (Sierra Morena).

AKNOWLEDGEMENTS

This study was developed by the IGME (Instituto Geológico y Minero de España, in Sevilla) in collaboration with the UPC (Universitat Politècnica de Catalunya, in Barcelona) and the IJA (Institut de Ciències de la Terra Jaume Almera, in Barcelona), between 2004 and 2008 in the framework of a research project focused on the stratigraphy and sedimentology of the Neogene and Quaternary deposits of the lower Guadalquivir basin. The authors wish to thank Drs. Emilio Custodio (UPC) and Vicente Gabaldón (IGME) for promoting this project and helping its development, and Drs. Jesús Galindo-Zaldíbar (Universidad de Granada) and Oriol Oms (Universitat Autònoma de Barcelona) for their critical reading of the first version of the manuscript. The authors also acknowledge Dr. A.D. Miall and other two anonymous reviewers, and the Editor, Dr. Brian Jones, for their comments, which greatly improve the manuscript.

REFERENCES

Armijo, R., Benkhelil, J., Bousquet, J.Cl., Estévez, A., Guiraud, R., Montenat, Ch., Pavillon, M.J., Philip, H., Sanz de Galdeano, C., Viguier, CL., 1977. Chapitre III, Les résultats de l’analyse structurale en Espagne. In: Grupe de recherche néotectonique de l’Arc de Gibraltar. L’histoire tectonique récent (Tortonien à Quaternaire) de l’Arc de Gibraltar et des bordures de la mer d’Alboran. Bull. Soc. Geol. France 7–19, 575–614.

Baceta, J.I., Pendón, J.G., 1999. Estratigrafía y arquitectura de facies de la Formación Niebla, Neógeno Superior, sector occidental de la cuenca del Guadalquivir. Rev. Soc. Geol. España 12, 419–438.

Bayán, B., Dolz, J., 1995. Las aguas superficiales y la marisma del Parque Nacional de Doñana. Revista de Obras Públicas 3340, 17–29.

Beaumont, Ch., Quinlan, G., Hamilton, J., 1988. Orogeny and stratigraphy: numerical models of the Paleozoic in the Eastern Interior of North America. Tectonics 7-3, 389-416.

Berastegui, X., Banks, C.J., Puig, C., Taberner, C., Waltham, D., Fernández, M., 1998. Later diapiric emplacement of Triassic evaporites at the southern margin of the Guadalquivir Basin, Spain. In: Mascle, A., Puigdefàbregas, C., Luterbacker, H.P., Fernández, M. (Eds.), Cenozoic Foreland Basins of Western Europe. Geological Society Special Publication 134, 49–68.

Borja, F., Díaz del Olmo, F., 1992. Eastern sector of the cliff at El Asperillo (Huelva coast, SW Spain): formation and chronology. MBSS Newsletter 14, 87–93.

Caratini, C., Viguier, C., 1973. Étude palynologique et sédimentologique des sables hologenes de la falaise littorale d'El Asperillo (province de Huelva). Estudios Geológicos 29, 325–328.

Carretero, M.I., Ruiz, F., Rodríguez-Ramírez, A., Cáceres, L., Rodríguez-Vidal, J., González-Regalado, M.L., 2002. The use of clay minerals and microfossils in palaeoenvironmental reconstruction: the Holocene littoral strand of Las Nuevas (Doñana Nacional Park) SW Spain. Clay Minerals 37, 93–103.

Catuneanu, O., 2004. Retroarc foreland systems evolution through time. Journal African Earth Sciences 38, 225-242.

Catuneanu, O., Sweet, A.R., 1999. Maastrichtian-Paleocene forland-basin stratigraphies, western Canada: a reciprocal sequence architecture. Can. J. Earth Sci. 36, 685-703.

Civis, J., Sierro, F.J., González-Delgado, J.A., Flores, J.A., Andrés, I., Porta, J., Valle, M.F., 1987. El Neógeno marino de la provincia de Huelva: antecendentes y definición de las unidades litoestratigráficas. Stud. Geol. Salmantina, special issue, pp 9–21.

Civis, J., Dabrio, C.J., González-Delgado, J.A., Goy, J.L., Ledesma, S., Pais, J., Sierro, F.J., Zazo, C., 2004. Cuenca del Guadalquivir. In: Vera, J.A. (Ed.), Geología de España. Madrid, SGE-IGME, pp 543–550.

Crampton, S.L., Allen, P.A., 1995. Recognition of forebulge unconformities associated with early stage foreland basin development: example from the North Alpine Foreland Basin. AAPG Bull. 79-10, 1495-1514.

Cruse, K., 1979. A review of water well drilling methods. Quarterly Journal of Engineering Geology 12, 79–95.

Dabrio, C.J., Borja, F., Zazo, C., Boersma, J.R., Lario, J., Goy, J.L., Polo, M.D., 1996. Dunas eólicas y facies asociadas pleistocenas y holocenas en el acantilado del Asperillo (Huelva). Geogaceta 20, 1089–1092.

De Celles, P.G., Giles, K.A., 1996. Foreland basin systems. Basin Research 8, 105-123.

FAO (1970) Estudio hidrogeológico de la Cuenca del Guadalquivir: informe técnico. 1 AGL: SF/SPA 9, Roma, unpublished report, pp 1-115.

Fernández, M., Berastegui, X., Puig, C., García-Castellanos, D., Jurado, M.J., Torné, M., Banks, C., 1998. Geophysical and geological constraints on the evolution of the Guadalquivir foreland basin, Spain. In: Mascle, A., Puigdefàbregas, C., Luterbacker, H.P., Fernández, M. (Eds.), Cenozoic Foreland Basins of Western Europe. Geological Society Special Publication 134, pp 29–48.

Fleming, P.B., Jordan, T.E., 1990. Stratigraphic modelling of foreland basins: interpreting thrust deformation and lithosphere rheology. Geology 18, 430-434.

Flor, G., 1990. Tipología de dunas eólicas. Procesos de erosió-sedimentación costera y evolución litoral de la provincia de Huelva (Golfo de Cádiz occidental, Sur de España). Estudios Geológicos 46, 99–109.

Flores-Hurtado, E., Rodríguez-Vidal, J., 1994. Rasgos morfotectónicos del interfluvio costero Guadiana-Guadalquivir (Golfo de Cádiz). In: Arnáez, J., García-Ruiz, J.M., Gómez-Villar, A. (Eds.), Geomorfología en España. Sociedad Española de Geomorfología. Logroño, pp 13–19.

Galindo-Zaldívar, J., González-Lodeiro, F., Jabaloy, A., 1993. Stress and palaeostress in the Betic-Rif cordillera (Miocene to the present). Tectonophysics 227, 105-126.

García-Castellanos, D., Fernández, M., Torné, M., 2002. Modeling the evolution of the Guadalquivir foreland basin (southern Spain). Tectonics 21, 1–17.

Gibbard, Ph.L., Head, M.J., Walker, M.J.C., Subcommission on Quaternary Stratigraphy, 2009. Formal ratification of the Quaternary System/Period and the Pleistocene Series/Epoch with a base at 2.58 Ma. Journal of Quaternary Science 25, 96-102.

González-Delgado, J.A., Civis, J., Dabrio, C.J., Goy, J.L., Ledesma, S., Pais, J., Sierro, F.J., Zazo, C., 2004. Cuenca del Guadalquivir. In: Vera, J.A. (Ed.), Geología de España. Madrid, SGE-IGME, pp 543–550.

Goy, J.L., Zazo, C., Dabrio, C.J., Lario, J., 1994. Fault controlled shifting shorelines in the Gulf of Cadiz since 20ky BP. 1º Simpósio sobre a margem continental ibérica atlântica, Lisboa. Abstracts, 24.

Goy, J.L., Zazo, C., Dabrio, C.J., Lario, J., Borja, F., Sierro, F., Flores, J.A., 1996. Global and regional factors controlling changes of coastlines in southern Iberia (Spain) during the Holocene. Quaternary Science Reviews 15, 773–780.

Gradstein, F.M., Ogg, J.G., Smith, A.G., Bleeker, W., Lourens, L.J., 2004. A new geological time scale, with special reference to Precambrian and Neogene. Episodes 27, 83–100.

Heller, P.L., Angevine, Ch.L., Winslow, N.S., Paola, Ch., 1988. Two-phase stratigraphic model of foreland-basin sequences. Geology 16, 501-504.

IGME, 1983. Hidrogeología del Parque Nacional de Doñana y su entorno. Servicio de Publicaciones del Ministerio de Industria y Energía, Madrid. pp 1-120.

IRYDA, 1976. Informe final de los sondeos de la zona regable de Almonte-Marismas (Huelva-Sevilla). Unpublished report, pp 1-100.

Kirschvink, J.L., 1980. The least-squares line and plane and the analysis of paleomagnetic data, Geophys. J. R. Astron. Soc. 62, 699–718.

Lario, J., Zazo, C., Plater, A.J., Goy, J.L., Dabrio, C.J., Borja, F., Sierro, F.J., Luque, L., 2001. Particle size and magnetic propierties of Holocene estuarine deposits from the Doñana National Park (SW Iberia): evidence of gradual and abrupt coastal sedimentation. Z. Geomorph. N. F. 45, 33–54

Lario, J., Zazo, C., Goy, J.L., Dabrio, C.J., Borja, F., Silva, P.G., Sierro, F., González, A., Soler, V., Yll, E., 2002. Changes in sedimentation trends in SW Iberia Holocene estuaries (Spain). Quaternary International 93–94, 171–176.

Leyva, F., Pastor, F., 1976. Mapa Geológico de España 1:50.000, 1017, El Abalario. IGME, Servicio de Publicaciones del Ministerio de Industria, Madrid.

Lourens, L.J., Hilgen, F.J., Shackleton, N.J., Laskar, J., Wilson, D.S., 2004. The Neogene period. In: Gradstein, F.N., Ogg, J.G., Smith, A.G. (Eds.), A Geologic Time Scale 2004. Cambridge University Press, pp 409–440.

Magne, J. and Viguier, Cl. (1974) Stratigraphie du Néogène marin “post-nappe” de l’Andalousie occdentale. *Mem. B.R.G.M.*, 78–2, 821–827.

Martínez del Olmo, W., García-Mojonero, C., Torrescusa, S., 2005. The Guadalquivir and Gulf of Cádiz gas basins (SW, Spain). Publ. Asociación de Geólogos y Geofísicos Españoles del Petroleo, 25 aniversario, 105–121.

Mayoral, E., Pendón J.G., 1986–87. Icnofacies y sedimentación en zona costera. Plioceno superior (?), litoral de Huelva. Acta Geológica Hispánica 21–22, 507–513.

Menanteau, L., 1979. Les marismas du Guadalquivir. Example de transformation d’un paisaje alluvial au cours du Quaternaire récent. Ph D Thesis, Université Paris-Sorbone, pp 1-154.

Morales, J., Serrano, I., Jabaloy, A., Galindo-Zaldívar, J., Zhao, D., Torcal, F., Vidal, F., González-Lodeiro, F., 1999. Active continental subduction beneath the Betic Cordillera and the Alboran Sea. Geology 27, 735-738.

Pendón, J.G., Rodríguez-Vidal, J., 1986–87. Caracteres sedimentológicos y geomorfológicos del Alto Nivel Aluvial cuaternario en el litoral de Huelva. Acta Geológica Hispánica 21–22, 107–111.

Perconig, E., Martínez-Díaz, C., 1977. Perspectivas petrolíferas de Andalucía Occidental. Boletín Geológico y Minero 88, 417–433.

Plint, A.G., Hart, B.S., Donaldson, W.S., 1993. Lithospheric flexure as a control on stratal geometry and facies distribution in Upper Cretaceous rocks of the Alberta foreland basin. Basin Research 5, 69-77.

Pozo, M., Carretero, M.I., Ruiz, F., Rodríguez-Vidal, J., Cáceres, L.M., Abad, M., 2008. Caracterización mineralógica de facies sedimentarias de edad Pleistoceno superior-Holoceno en el Parque Nacional de Doñana (Huelva). Implicaciones paleoambientales. Geo-Temas 10, 953–956.

Pozo, M., Ruiz, F., Carretero, M.I., Rodríguez-Vidal, J., Cáceres, L.M., Abad, M., González-Regalado, M.L., 2010. Mineralogical assemblages, geochemistry and fossil associations of Pleistocene-Holocene complex siliciclastic deposits from the Southwestern Doñana National Park (SW Spain): A palaeoenvironmental approach. Sedimentary Geology 225, 1-18.

Quinlan, G.M., Beaumont, Ch., 1984. Appalachian thrusting, lithosphere flexure, and the Paleozoic stratigraphy of the Eastern Interior of North America. Can. J. Earth Sci. 21, 973-996.

Rodríguez-Ramírez, A., 1998. *Geomorfología del Parque Nacional de Doñana y su entorno*. Publ. Ministerio de Medio Ambiente, Organismo Autónomo Parques Nacionales, pp 1-146.

Rodríguez-Ramírez, A., Rodríguez-Vidal, J., Cáceres, L.M., Clemente, L., Belluomini, G., Manfra, L., Improta, S., de Andrés, J.R., 1996a. Evolución costera de la desembocadura del Guadalquivir en los últimos 6000 años (SW de España). Geogaceta 20, 1086–1088.

Rodríguez-Ramírez, A., Rodríguez-Vidal, J., Cáceres, L., Clemente, L., Belluomini, G., Manfra, L., Improta, S., de Andrés, J.R., 1996b. Recent coastal evolution of the Doñana Nacional Park (SW Spain). Quaternary Science Reviews 15, 803–809.

Rodríguez-Ramírez, A., Cáceres, L.M., Ruiz, F., González-Regalado, M.L., Muñiz, F., Rodríguez-Vidal, J., Abad, M., Carretero, M.I., 2001. Génesis y caracterización del cordón estuarino de Las Nuevas (P.N. de Doñana). Geogaceta 29, 103–106.

Rodríguez-Vidal, J. (1989) El inicio de la red fluvial cuaternaria en el sector occidental de la Depresión del Guadalquivir. In: *El Cuaternario en Andalucía Occidental* (Ed. by F. Díaz del Olmo and J. Rodríguez Vidal). AEQUA Monografías, 1, 27–31.

Ruiz-Muñoz, F., González-Regalado-Montero, M.L., Redondo-Sanz, J.L., 1997. Guía de fósiles del sur de la provincia de Huelva. Diputación de Huelva, pp 1-205.

Ruiz, F., Rodríguez-Ramírez, A., Cáceres, L.M., Rodríguez-VidaL, J., Carretero, M.I., Clemente, L., Muñoz, J.M., Yañez, C., Abad, M., 2004. Late Holocene evolution of the Southwestern Doñana National Park (Guadalquivir Estuary, SW Spain): a multivariable approach. Palaeogeogr, Palaeoclimatol, Palaeoecol 204, 47–64.

Ruiz, F., Rodríguez-Ramírez, A., Cáceres, L.M., Rodríguez-Vidal, J., Carretero, M.I., Abad, M., Olias, M., Pozo, M., 2005. Evidence of high-energy events in the geological record: Mid-holocene evolution of the Southwestern Doñana National Park (SW Spain). Palaeogeogr, Palaeoclimatol, Palaeoecol 229, 212–229.

Salvany, J.M., 2004. Tilting neotectonics of the Guadiamar drainage basin, SW Spain. Earth Surface Processes and Landforms 29, 145–160.

Salvany, J.M., Custodio, E., 1995. Características litoestratigráficas de los depósitos plio-cuaternarios del bajo Guadalquivir en el área de Doñana: implicaciones hidrogeológicas. Rev. Soc. Geol. de España 8, 21–31.

Salvany, J.M., Carrera, J., Bolzicco, J., Mediavilla, C., 2004. Pitfalls in the geological characterization of alluvial deposits: site investigation for reactive barrier installation at Aznalcóllar, Spain. Quarterly Journal of Engineering Geology and Hydrogeology 37, 141–154.

Sanz de Galdeano, C., Vera, J.A., 1992. Stratigraphic record and palaeogeographical context of the Neogene basins in the Betic Cordillera, Spain. Basin Research 4, 21-36.

Sierro, F.J. (1985) Estudio de los foraminíferos plantónicos, bioestratigrafía y cronoestratigrafía del Mio-Plioceno del borde occidental de la Cuenca del Guadalquivir (SO de España). *Studia Geologica Salmanticensia*, 21, 7–85.

Sierro, F.J., González-Delgado, J.A., Dabrio, C.J., Flores, J.A., Civis J., 1996. Late Neogene depositional sequences in the foreland basin of Guadalquivir (SW Spain). In: Friend, P.F., C.J. Dabrio, C.J. (Eds.), Tertiary basins of Spain, the stratigraphic record of crustal kinematics. World and Regional Geology 6. Cambridge University Press, pp 339–345.

Sinclair, H.D., Coakley, B.J., Allen, P.A., Watt, A.B., 1991. Simulation of foreland basin stratigraphy using a diffusion model of mountain belt uplift and erosion: an example from the Central Alps, Switzerland. Tectonics 10-3, 599-620.

Tankard, A.J., 1986. Depositional response to foreland deformation in the Carboniferous of Eastern Kentucky. *AAPG Bull.* 70-7: 853-868.

Torres-Perezhidalgo, T., Fernández-Luanco, M.C., Leyva-Cabello, F., Granados, L.F., Martínez-Fresneda, F., Pan-Arana, T., Antón-Alfonso, S., 1977a. Mapa Geológico de España 1:50.000, hoja 1001, Almonte. IGME, Servicio de Publicaciones del Ministerio de Industria, Madrid.

Torres-Perezhidalgo, T., Fernández-Luanco, M.C., Leyva-Cabello, F., Granados, L.F., Martínez-Fresneda, F., Borragán-Pastor, J., Antón-Alfonso, S., 1977b. Mapa Geológico de España 1:50.000, hoja 1002, Dos Hermanas. IGME, Servicio de Publicaciones del Ministerio de Industria, Madrid.

Viguier, C., 1977. Les grands traits de la tectonique du basin néogène du Bas Guadalquivir. Boletín Geológico Minero 88, 39–44.

Zazo, C., Goy, J.L., Somoza, L., Dabrio, C.J., Belluomini, G., Improta, S., Lario, J., Bardají, T., Silva, P.G., 1994. Holocene sequence of sea-level fluctuations in relation to climatic trends in the Atlantic-Mediterranean linkage coast. Journal of Coastal Research 10, 933–945.

Zazo, C., Dabrio, C.J., González, A., Sierro, F., Yll, E.I., Goy, J.L., Luque, L., Pantaleón-Cano, J., Soler, V., Roure, J., Lario, J., Hoyos, M., Borja, F., 1999a. The record of the latter glacial and interglacial periods in the Guadalquivir marshlands (Mari López drilling, SW Spain). Geogaceta 26, 119–122.

Zazo, C., Dabrio, C.J., Borja, J.L., Lezine, A.M., Lario, J., Polo, M.D., Hoyos, M., Boersma, J.R., 1999b. Pleistocene and Holocene aeolian facies along the Huelva coast (sothern Spain): climatic and neotectonic implications. Geologie en Mijnbouw 77, 209–224.

Zazo, C., Mercier, N., Silva, P.G., Dabrio, C.J., Goy, J.L., Roquero, E., Soler, V., Borja, F., Lario, J., Polo, D., de Luque, L., 2005. Landscape evolution and geodynamic control in the Gulf of Cadiz (Huelva coast, SW Spain) during the Late Quaternary. Geomorphology 68, 269–290.

Zazo, C., Dabrio, C.J., Goy, J.L., Lario, J., Cabero, A., Silva, P.G., Bardají, T., Mercier, N., Borja, F., Roquero, E., 2008. The coastal archives of the last 15ka in the Atlantic-Mediterranean Spanish linkage area: Sea level and climatic changes. Quaternary International 181, 72–87.

Zijderveld, J.D.A., 1967. Demagnetization of rocks: analysis of results. In: Collinson D.W., Creer, K.M., Runcorn, S.K. (Eds.), Methods in Palaeomagnetism. Elsevier, Amsterdam, pp 254–286.

FIGURE CAPTIONS

Table 1. Study boreholes drilled by IGME in the Abalario high and Guadalquivir marshlands of the lower Guadalquivir basin.

Table 2. Radiocarbon ages of samples from the studied boreholes in the Guadalquivir marshlands.

Figure 1. Geological map of the lower Guadalquivir basin, and location of study boreholes and cross-sections in figures 2, 3, 4 and 5 (map adapted from IGME's 1:50.000 geological maps).

Figure 2. Lithologic logs and correlation of study boreholes in cross-sections 1 and 2. See Figure 1 for locations.

Figure 3. Lithologic logs and correlation of study boreholes in cross-sections 3 and 4. See Figure 1 for locations and Figure 2 for legend.

Figure 4. Lithologic logs and correlation of study boreholes in cross-section 5. See Figure 1 for locations and Figure 2 for legend.

Figure 5. Lithostratigraphic cross-sections of the Plio-Quaternary formations through the Abalario and the Guadalquivir marshlands as derived from the study boreholes described in Figures 2, 3 and 4. See Figure 1 for locations.

Figure 6. Demagnetization plots representative of the different formations studied. Grey lines represent the linear fit to calculated ChRM directions. Demagnetization plots are in geographic coordinates with arbitrary cardinal points, and temperature steps are in ºC. The quality of ChRM directions is indicated. Dark lines indicate the fit to the ChRM directions. Solid (open) circles represent projections in the horizontal (vertical) plane.

Figure 7. Sequence of polarity changes established for Lebrija borehole and its correlation to the ATNTS2004 (Lourens et al., 2004; Gradstein et al., 2004). The age of the Pliocene-Pleistocene boundary is updated according to Gibbard et al. (2009). Mean accumulation rates between main reversals (black dots) are given in cm/Kyr. The undulated line indicates the position of a sedimentary gap or hiatus. The upper arrow indicates the position of the oldest sample with an age that is within the range of radiocarbon dating, and the lower one indicates the position of a sample with an age that is beyond that range. The estimated ages for the base of the Lebrija Formation (3.7 Ma), the long hiatus (1.6-0.3 Ma), the base of the Marismas Formation (85-110 ka), and the position of the Pleistocene-Holocene boundary (11.5 ka) have been indicated using bold labels.

Figure 8. Lithostratigraphic cross-sections through four areas of the lower Guadalquivir basin, based on the correlation of representative hydrogeologic boreholes (vertical lines) drilled in the region.

Figure 9. Correlation between the Guadiamar alluvial terraces and the LE borehole of the Guadalquivir marshlands. Upper part: longitudinal cross-section from the Guadiamar Valley to the LE borehole, adapted from Salvany (2004). Lower part: schematic cross-section (without scale) of the Guadiamar alluvial terraces representative of the northern half of the valley, and radiocarbon ages from Salvany (2004) and Salvany et al. (2004)

Figure 10. Schematic cross-sections (without scale) and paleogeographic maps illustrating the sedimentary evolution of the lower Guadalquivir basin during the Upper Pliocene and Quaternary.

Figure 1

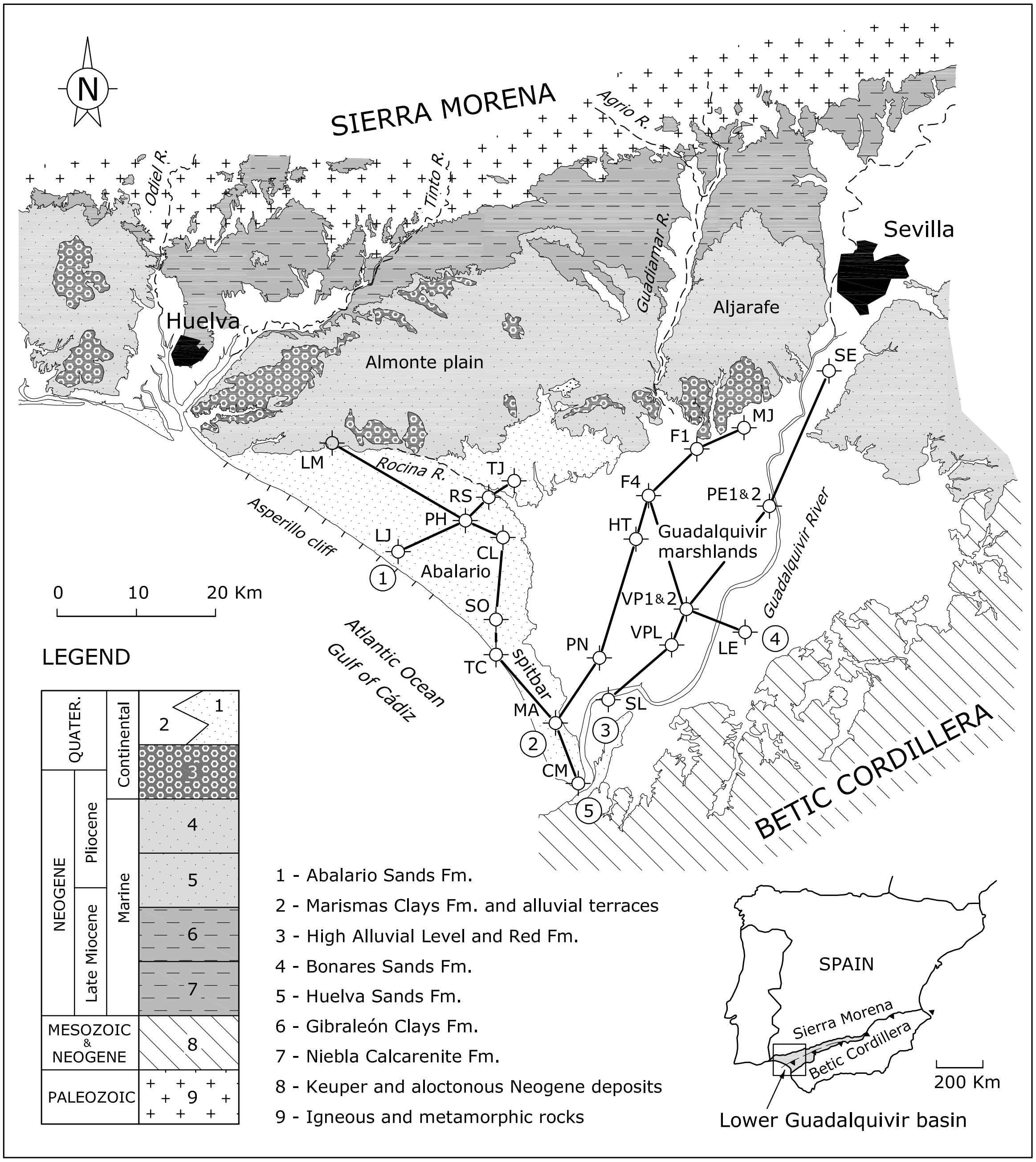

N
SIERRA MORENA
Odiel R.
Tinto R.
Agrio R.
Guadiamar R.
Sevilla
Huelva
Aljarafe
Almonte plain
SE
MJ
F1
LM
Rocina R.
TJ
F4
PE1&2
RS
PH
HT
Guadalquivir marshlands
Asperillo cliff
LJ
CL
1
Abalario
Guadalquivir River
0
10
20 Km
SO
VP1&2
VPL
LE
4
Atlantic Ocean
Gulf of Cádiz
PN
TC
spitbar
MA
SL
3
2
CM
5
BETIC CORDILLERA
LEGEND
QUATER.
NEOGENE
Pliocene
Late Miocene
Continental
Marine
MESOZOIC & NEOGENE
PALEOZOIC
1 - Abalario Sands Fm.
2 - Marismas Clays Fm. and alluvial terraces
3 - High Alluvial Level and Red Fm.
4 - Bonares Sands Fm.
5 - Huelva Sands Fm.
6 - Gibraleón Clays Fm.
7 - Niebla Calcarenite Fm.
8 - Keuper and aloctonous Neogene deposits
9 - Igneous and metamorphic rocks
SPAIN
Sierra Morena
Betic Cordillera
200 Km
Lower Guadalquivir basin

Figure 2

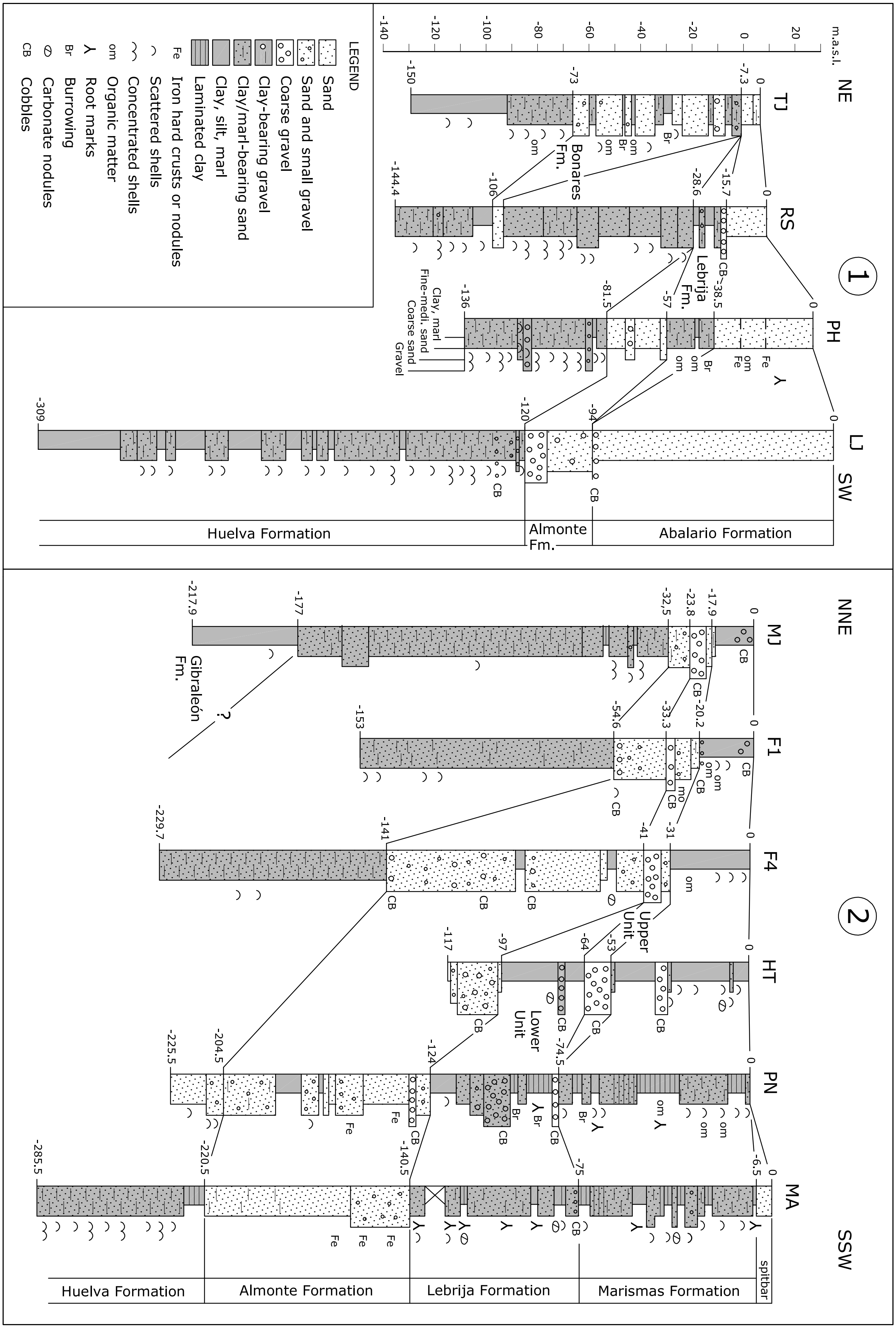

NE
SW
NNE
SSW
1
2
m.a.s.l.
TJ
RS
PH
LJ
MJ
F1
F4
HT
PN
MA
Bonares Fm.
Lebrija Fm.
Gibraleón Fm.
Upper Unit
Lower Unit
Clay, marl
Fine-medi. sand
Coarse sand
Gravel
Huelva Formation
Almonte Fm.
Abalario Formation
Almonte Formation
Lebrija Formation
Marismas Formation
spitbar
LEGEND
Sand
Sand and small gravel
Coarse gravel
Clay-bearing gravel
Clay/marl-bearing sand
Clay, silt, marl
Laminated clay
Fe Iron hard crusts or nodules
Scattered shells
Concentrated shells
om Organic matter
Root marks
Br Burrowing
Carbonate nodules
CB Cobbles

Figure 3

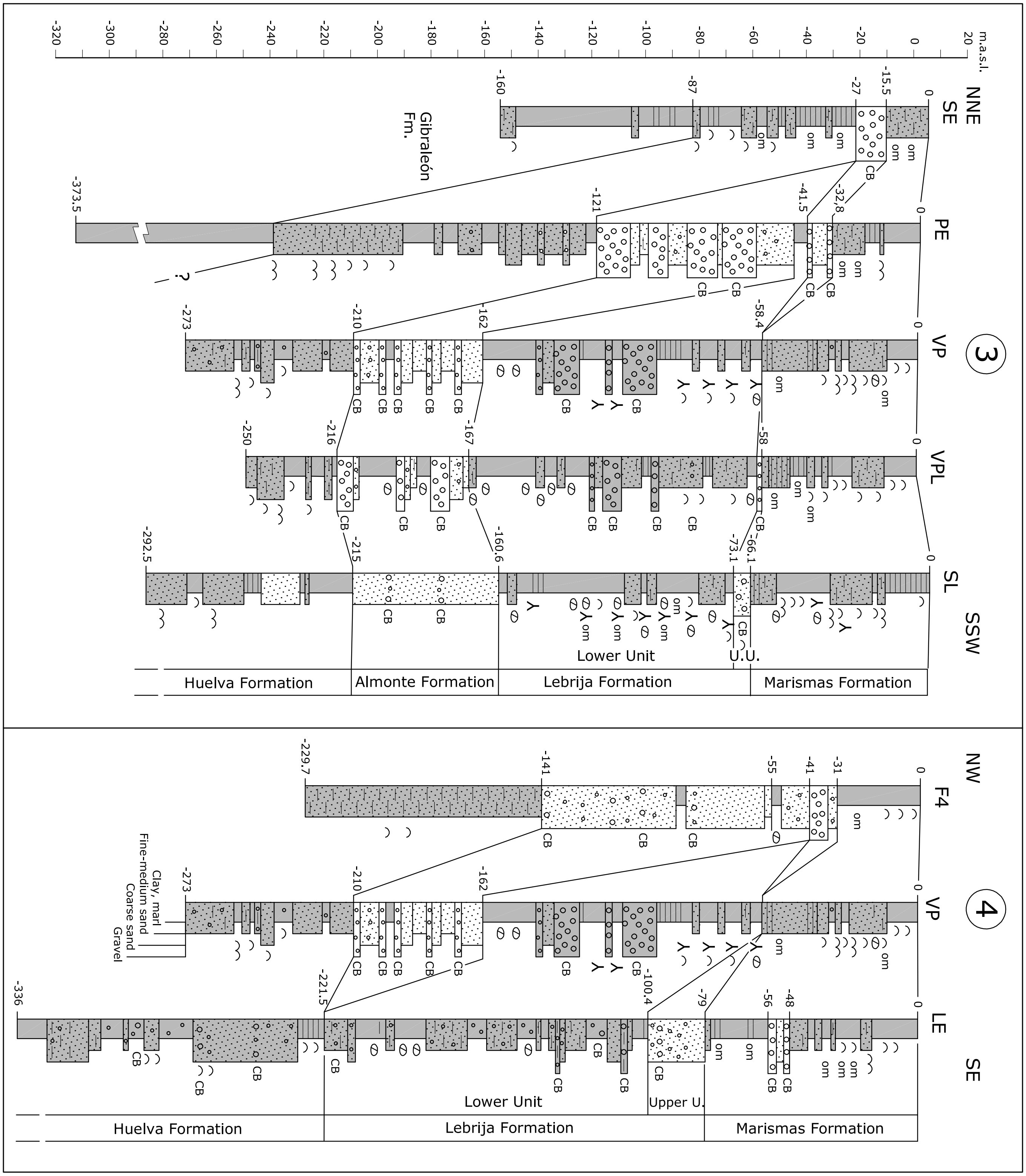

m.a.s.l.
3
NNE
SE
PE
VP
VPL
SL
SSW
Gibraleón Fm.
Lower Unit
U.U.
Huelva Formation
Almonte Formation
Lebrija Formation
Marismas Formation
4
NW
F4
VP
LE
SE
Clay, marl
Fine-medium sand
Coarse sand
Gravel
Lower Unit
Upper U.
Huelva Formation
Lebrija Formation
Marismas Formation

Figure 4

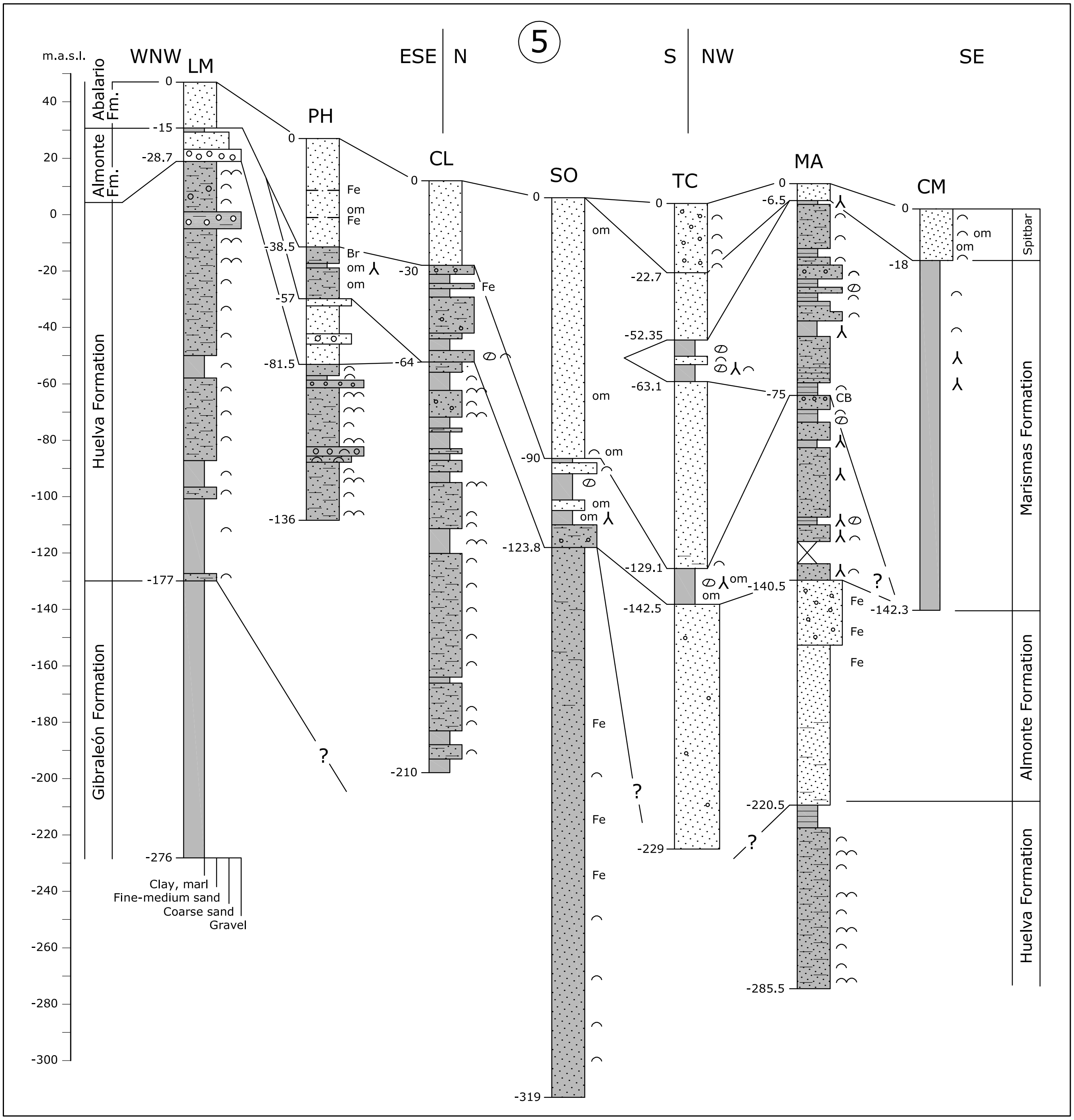
5
m.a.s.l.
WNW
LM
PH
ESE
N
CL
SO
S
NW
TC
MA
CM
SE
Abalario Fm.
Almonte Fm.
Huelva Formation
Gibraleón Formation
Spitbar
Marismas Formation
Almonte Formation
Huelva Formation
Clay, marl
Fine-medium sand
Coarse sand
Gravel
Fe
om
Br
CB
?
0
-15
-28.7
-177
-276
-38.5
-57
-81.5
-136
-30
-64
-210
-90
-123.8
-319
-22.7
-52.35
-63.1
-129.1
-142.5
-229
-6.5
-75
-140.5
-220.5
-285.5
-18
-142.3
40
20
-20
-40
-60
-80
-100
-120
-140
-160
-180
-200
-220
-240
-260
-280
-300

Figure 5

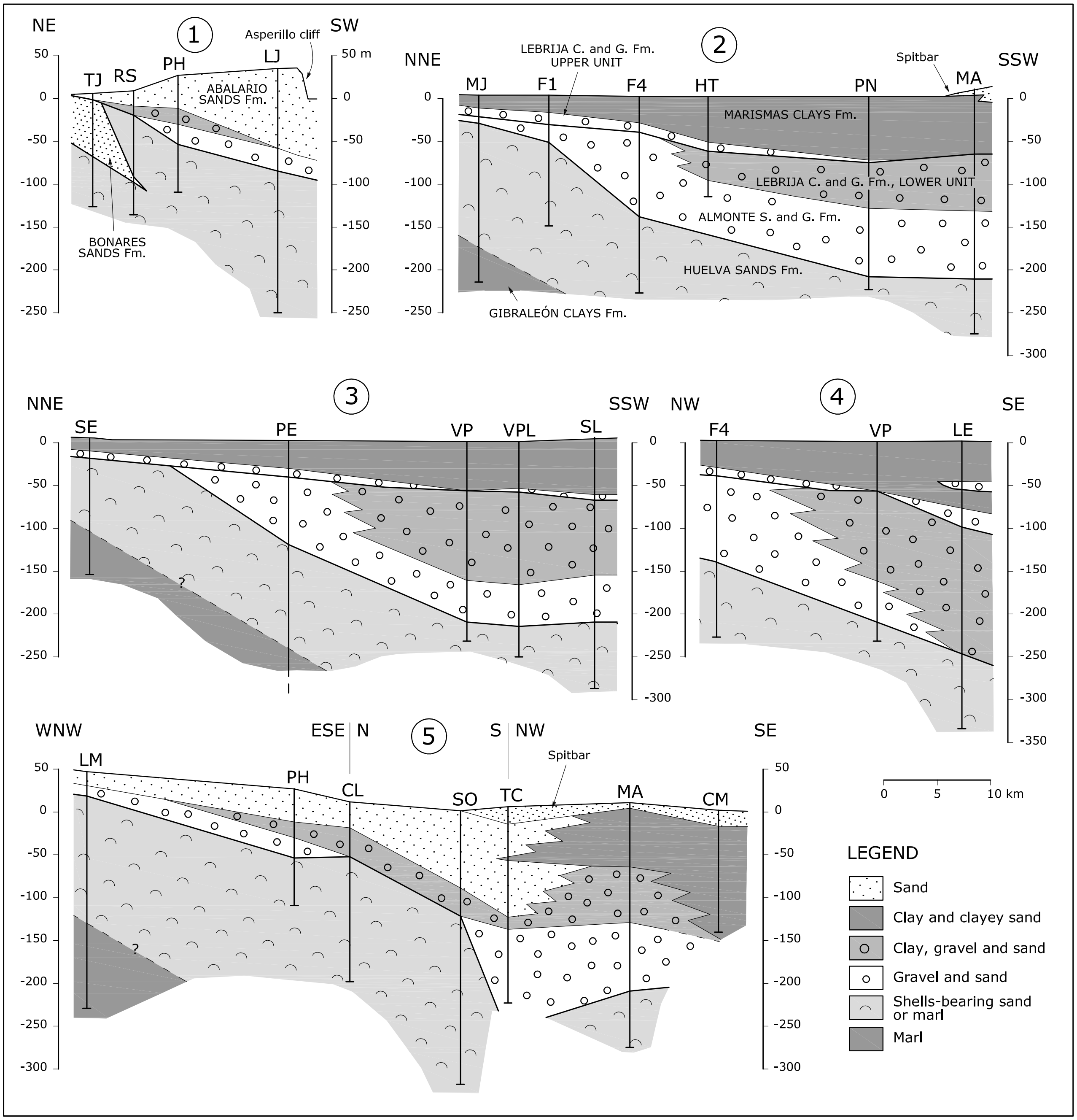

1
NE
SW
Asperillo cliff
TJ
RS
PH
LJ
ABALARIO SANDS Fm.
BONARES SANDS Fm.
50 m
2
NNE
SSW
LEBRIJA C. and G. Fm. UPPER UNIT
Spitbar
MJ
F1
F4
HT
PN
MA
MARISMAS CLAYS Fm.
LEBRIJA C. and G. Fm., LOWER UNIT
ALMONTE S. and G. Fm.
HUELVA SANDS Fm.
GIBRALEÓN CLAYS Fm.
3
NNE
SSW
SE
PE
VP
VPL
SL
4
NW
SE
F4
VP
LE
5
WNW
ESE
N
S
NW
SE
Spitbar
LM
PH
CL
SO
TC
MA
CM
0
5
10 km
LEGEND
Sand
Clay and clayey sand
Clay, gravel and sand
Gravel and sand
Shells-bearing sand or marl
Marl

Figure 6

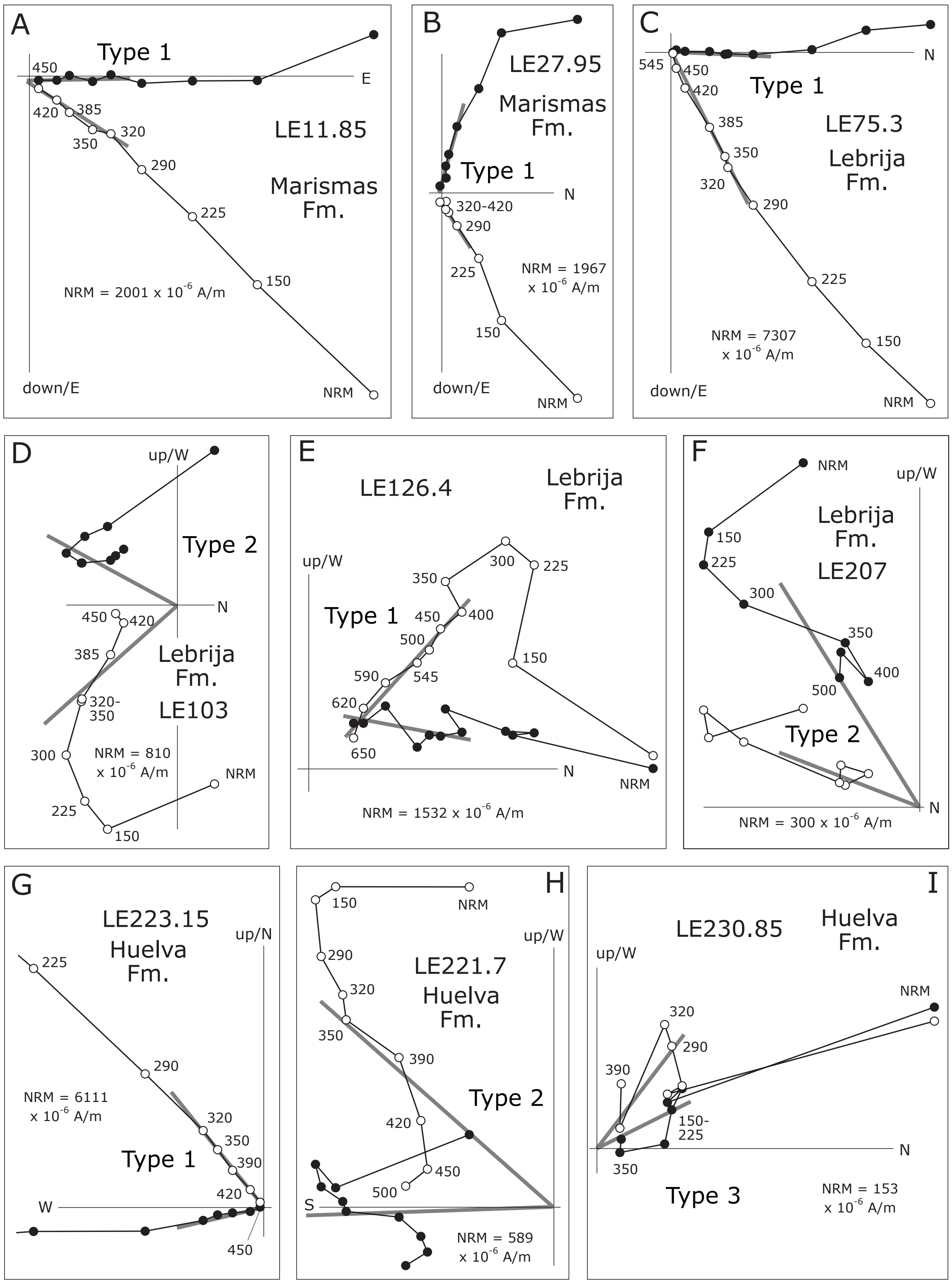

A
Type 1
LE11.85
Marismas Fm.
NRM = 2001 x 10^-6 A/m
down/E
E
450
420
385
350
320
290
225
150
NRM
B
LE27.95
Marismas Fm.
Type 1
N
320-420
290
225
150
NRM = 1967 x 10^-6 A/m
down/E
NRM
C
Type 1
LE75.3
Lebrija Fm.
N
545
450
420
385
350
320
290
225
150
NRM = 7307 x 10^-6 A/m
down/E
NRM
D
up/W
Type 2
N
450
420
385
Lebrija Fm.
LE103
320-350
300
NRM = 810 x 10^-6 A/m
NRM
225
150
E
LE126.4
Lebrija Fm.
up/W
Type 1
300
225
350
400
450
500
150
590
545
620
650
N
NRM
NRM = 1532 x 10^-6 A/m
F
NRM
up/W
150
Lebrija Fm.
225
LE207
300
350
400
500
Type 2
N
NRM = 300 x 10^-6 A/m
G
LE223.15
Huelva Fm.
up/N
225
290
NRM = 6111 x 10^-6 A/m
320
350
Type 1
390
420
W
450
H
150
NRM
up/W
290
LE221.7
Huelva Fm.
320
350
390
Type 2
420
450
500
S
NRM = 589 x 10^-6 A/m
I
LE230.85
Huelva Fm.
up/W
NRM
320
290
390
150-225
N
350
Type 3
NRM = 153 x 10^-6 A/m

Figure 7

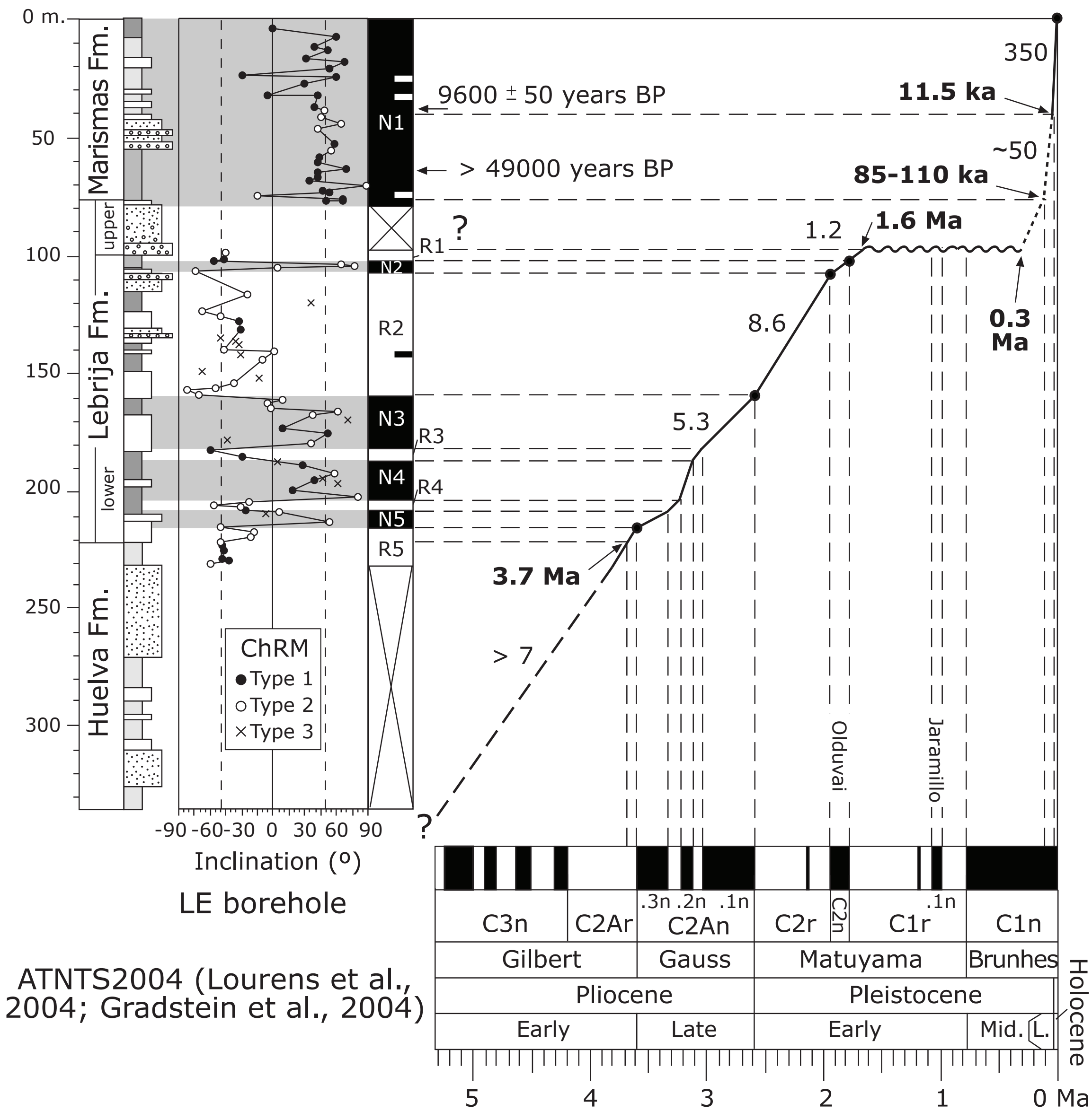
0 m.
50
100
150
200
250
300
Marismas Fm.
upper
Lebrija Fm.
lower
Huelva Fm.
N1
N2
R1
R2
N3
R3
N4
R4
N5
R5
?
9600 ± 50 years BP
> 49000 years BP
ChRM
Type 1
Type 2
Type 3
-90 -60-30 0 30 60 90
Inclination (º)
LE borehole
350
11.5 ka
~50
85-110 ka
1.2
1.6 Ma
0.3
Ma
8.6
5.3
3.7 Ma
> 7
Olduvai
Jaramillo
C3n
C2Ar
.3n .2n .1n
C2An
C2r
C2n
.1n
C1r
C1n
Gilbert
Gauss
Matuyama
Brunhes
Pliocene
Pleistocene
Holocene
Early
Late
Early
Mid.
L.
5
4
3
2
1
0 Ma
ATNTS2004 (Lourens et al., 2004; Gradstein et al., 2004)

Figure 8

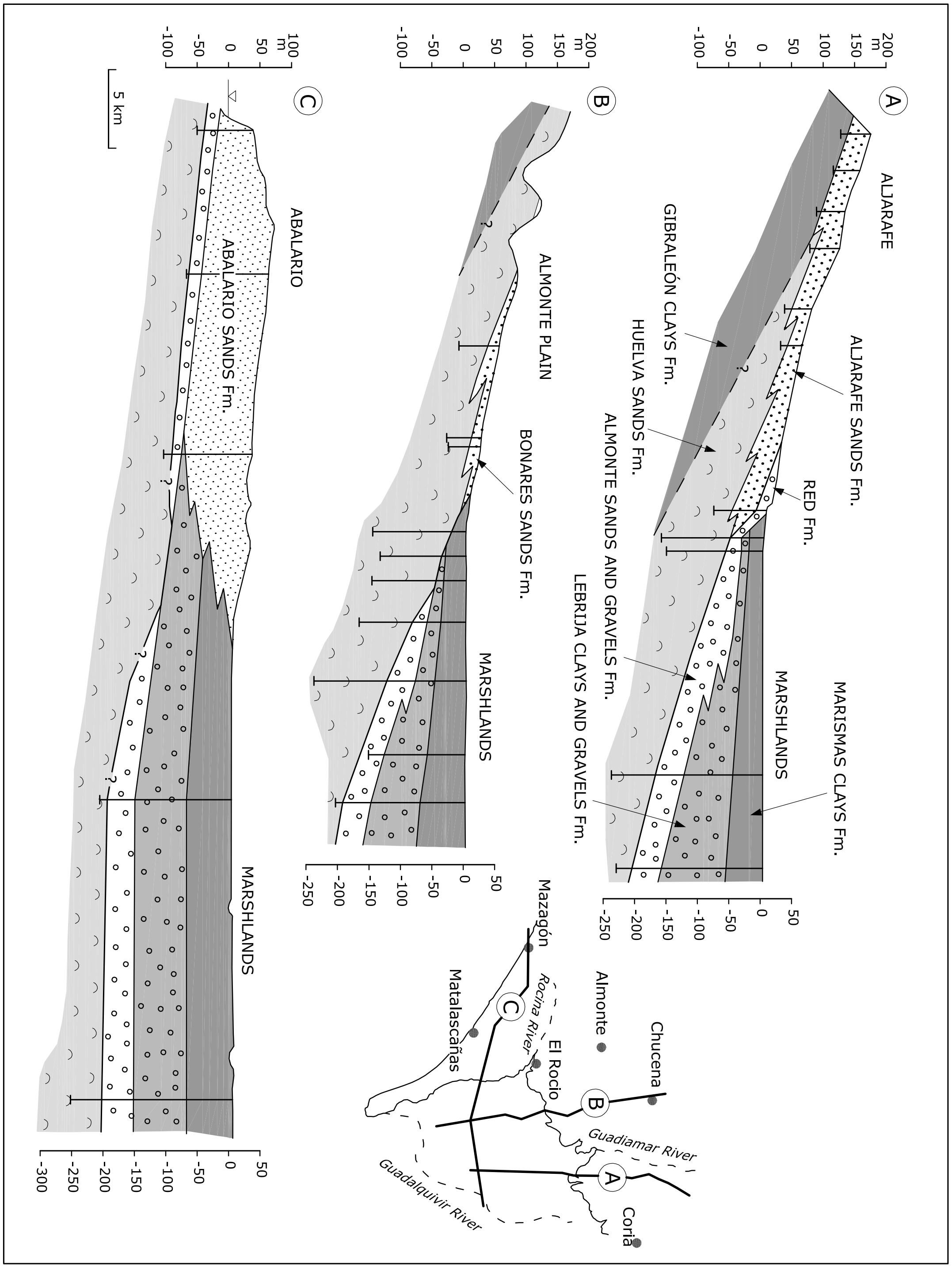

A
ALJARAFE
GIBRALEÓN CLAYS Fm.
ALJARAFE SANDS Fm.
HUELVA SANDS Fm.
ALMONTE SANDS AND GRAVELS Fm.
RED Fm.
LEBRIJA CLAYS AND GRAVELS Fm.
MARSHLANDS
MARISMAS CLAYS Fm.
B
ALMONTE PLAIN
BONARES SANDS Fm.
MARSHLANDS
C
ABALARIO
ABALARIO SANDS Fm.
MARSHLANDS
5 km
m
Mazagón
Almonte
Chucena
Matalascañas
Rocina River
El Rocío
Guadiamar River
Guadalquivir River
Coria

Figure 9

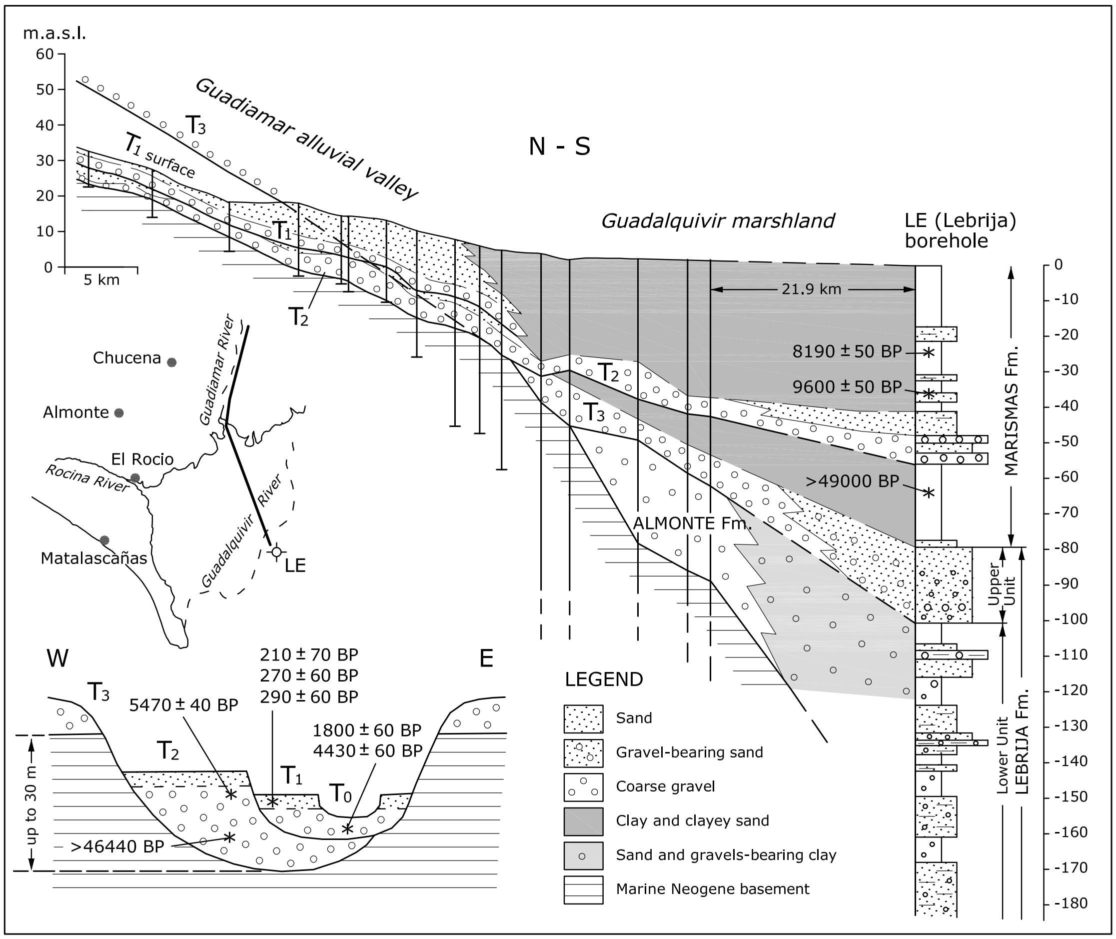

m.a.s.l.
60
50
40
30
20
10
0
5 km
T3
T1 surface
T1
T2
Guadiamar alluvial valley
N - S
Guadalquivir marshland
LE (Lebrija) borehole
21.9 km
8190 ± 50 BP
9600 ± 50 BP
>49000 BP
T2
T3
ALMONTE Fm.
MARISMAS Fm.
Upper Unit
Lower Unit
LEBRIJA Fm.
0
-10
-20
-30
-40
-50
-60
-70
-80
-90
-100
-110
-120
-130
-140
-150
-160
-170
-180
Chucena
Almonte
El Rocio
Rocina River
Matalascañas
Guadiamar River
Guadalquivir River
LE
W
E
T3
T2
T1
T0
5470 ± 40 BP
210 ± 70 BP
270 ± 60 BP
290 ± 60 BP
1800 ± 60 BP
4430 ± 60 BP
>46440 BP
up to 30 m
LEGEND
Sand
Gravel-bearing sand
Coarse gravel
Clay and clayey sand
Sand and gravels-bearing clay
Marine Neogene basement

Figure 10

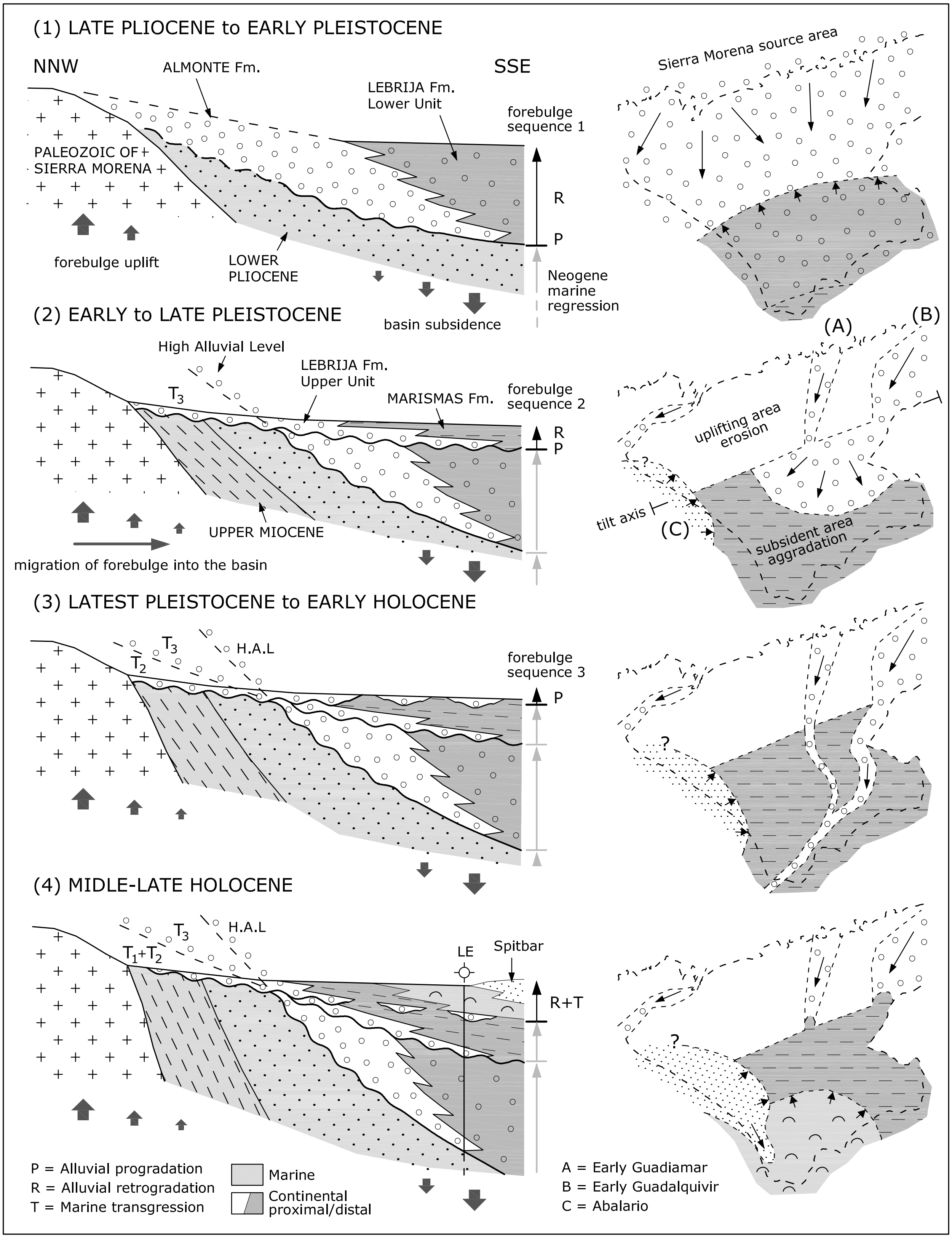

(1) LATE PLIOCENE to EARLY PLEISTOCENE
NNW
ALMONTE Fm.
SSE
LEBRIJA Fm. Lower Unit
forebulge sequence 1
PALEOZOIC OF SIERRA MORENA
R
P
forebulge uplift
LOWER PLIOCENE
Neogene marine regression
basin subsidence
Sierra Morena source area
(2) EARLY to LATE PLEISTOCENE
High Alluvial Level
LEBRIJA Fm. Upper Unit
T_3
MARISMAS Fm.
forebulge sequence 2
UPPER MIOCENE
migration of forebulge into the basin
(A)
(B)
uplifting area erosion
tilt axis
(C)
subsident area aggradation
(3) LATEST PLEISTOCENE to EARLY HOLOCENE
T_3
H.A.L
T_2
forebulge sequence 3
P
?
(4) MIDLE-LATE HOLOCENE
H.A.L
T_3
T_1+T_2
LE
Spitbar
R+T
P = Alluvial progradation
R = Alluvial retrogradation
T = Marine transgression
Marine
Continental proximal/distal
A = Early Guadiamar
B = Early Guadalquivir
C = Abalario

Table 1

Click here to download Table: Table 1.eps

Borehole name and year of drilling	Label	Length (m)	X (UTM*)	Y (UTM*)	Z (m)	Intervals of continuous core sampling (CCS) (mbs***)	Average of CCS	Drilling method**
Feder-1 (Casa Nieves), 1999	F1	153	747853	4119188	4	0-33.25, 46-57.6	29.3%	DCRM
Feder-4 (Hato Ratón), 1999	F4	229.7	742222	4112907	3	0-229.7	100%	DCRM
Cuartel de Malhandar, 1999	CM	142.35	736012	4076023	2	0-142.35	100%	DCRM
Corral de La Marta, 2000	MA	289.5	732572	4083562	11	0-289.5	100%	DCRM
Palacio de Las Nuevas, 2000	PN	225.5	737503	4092111	3	0-144.5	64.1%	DCRM
Sanlúcar, 2000	SL	292.5	738989	4086966	6	0-160.6, 214-235, 248.5-256.5	64.8%	DCRM
Torre Carbonero, 2001	TC	229	724502	4091592	4	0-97, 129-141.2	47.7%	DCRM
Laguna de Santa Olalla, 2001	SO	319	724184	4096029	6	0-131	41%	DCRM
Veta La Palma-1, 2002	VP1	156.5	747956	4099016	2	0-102, 111-129.7, 150-156.6	81.3%	DCRM
Veta La Palma-2, 2002	VP2	273	747956	4099016	2	145-273	46.9%	DCRM
Cortijo de La Marmoleja, 2002	MJ	217.9	753589	4122284	4	0-40.3, 73.2-149.5, 177-217.9	72.3%	DCRM
Poblado Escobar-1, 2003	PE1	264.5	757464	4112668	3	0-264.5	100%	DCRM
Poblado Escobar-2, 2004	PE2	373.5	757464	4112668	3	279-319, 345-373.5	18.3%	DCRM
El Sequero, 2004	SE	159.3	763750	4130161	6	0-115.7, 153-159.3	76.6%	DCRM
Lebrija, 2005	LE	336	755553	4096658	2	0-86, 96-232.3	66.2%	DCRM
Laguna del Jaral, 2006	LJ	309	711300	4103650	35	0-93.9, 120-309	91.5%	DCRM
Huerta Tejada, 2006	HT	117	741830	4106482	1	without CCS	0%	RCRM
La Matilla, 2006	LM	276	702052	4116679	47	0-276	100%	DCRM
Rocina Sur, 2007	RS	144.4	722168	4111287	9	0-144.4	100%	DCRM
Tarajales, 2007	TJ	150	725220	4113567	6	0-150	100%	DCRM
Pequeña Holanda, 2007	PH	136.2	719463	4108137	27	0-136.2	100%	DCRM
Laboratorio Veta La Palma, 2007	VPL	250	746452	4094395	3	without CCS	0%	RCRM
Casa del Lobo, 2008	CL	210	724328	4106357	12	without CCS	0%	RCRM

* UTM coordinates Zone 29N

** DCRM = Direct circulation rotary method; RCRM = Reverse circulation rotary method by large roller bit

*** mbs = meters bellow the surface

Table 2
Click here to download Table: Table 2.eps

Borehole	Depth	Material	analysis	Conventional ^{14}C age	$^{13}C/^{12}C$ $^{0}/_{00}$	^{14}C calibrated age	Laboratory*
LE	-24.25	peat	AMS	8190+/-50 BP		7340-7060 BC	P.R.
LE	-24.60	peat	AMS	8360+/-50 BP		7550-7300 BC	P.R.
LE	-25.40	peat	AMS	8640+/-50 BP		7760-7570 BC	P.R.
LE	-34.45	peat	AMS	9520+/-50 BP		9140-8700 BC	P.R.
LE	-35.50	peat	AMS	9830+/-40 BP		9370-9240 BC	P.R.
LE	-37.30	peat	AMS	9520+/-50 BP		9140-8700 BC	P.R.
LE	-37.60	peat	AMS	9600+/-50 BP		9220-8800 BC	P.R.
LE	-63.00	peat	AMS	>49000 BP			P.R.
VP	-51.50	peat	AMS	45460+/-1900 BP	-27.2		B.A.
PE	-28.90	charred	AMS	8320+/-60 BP	-25.1	7530-7180 BC	B.A.
SE	-8.00	charred	Radiom. Ext.	890+/-60 BP	-21.9	1020-1270 AD	B.A.
PN	-17.50	wood	AMS	7590+/-50 BP	-23.5	6480-6390 BC	B.A.
PN	-35.50	peat	AMS	>46000 BP	-27.5		B.A.
CM	-12.50	peat	AMS	3660+/-40 BP	-27.7	2140-1920 BC	B.A.
TC	-58.30	charred	AMS	29880+/-280 BP	-25.7		B.A.
TC	-131.00	peat	AMS	>46000 BP	-14.9		B.A.
TC	-142.45	peat	AMS	>44320 BP	-28.0		B.A.

* P.R. = Poznan Radiocarbon Laboratory, Poland; B.A. = Beta Analytic Inc., USA